HYBRID GEOMETRIC FEEDBACK CONTROL OF THREE-DIMENSIONAL BIPEDAL ROBOTIC WALKERS WITH KNEES AND FEET

A Thesis

by

RYAN WESLEY SINNET

Submitted to the Office of Graduate Studies of
Texas A&M University
in partial fulfillment of the requirements for the degree of

MASTER OF SCIENCE

May 2011

Major Subject: Mechanical Engineering

HYBRID GEOMETRIC FEEDBACK CONTROL OF THREE-DIMENSIONAL BIPEDAL ROBOTIC WALKERS WITH KNEES AND FEET

A Thesis

by

RYAN WESLEY SINNET

Submitted to the Office of Graduate Studies of
Texas A&M University
in partial fulfillment of the requirements for the degree of

MASTER OF SCIENCE

Approved by:

Chair of Committee,	Aaron D. Ames
Committee Members,	Gholamreza Langari
	Richard J. Malak
	Robin R. Murphy
Head of Department,	Dennis O'Neal

May 2011

Major Subject: Mechanical Engineering

ABSTRACT

Hybrid Geometric Feedback Control of
Three-Dimensional Bipedal Robotic Walkers
with Knees and Feet. (May 2011)
Ryan Wesley Sinnet, B.S., California Institute of Technology
Chair of Advisory Committee: Dr. Aaron D. Ames

This thesis poses a feedback control method for obtaining humanlike bipedal walking on a human-inspired hybrid biped model. The end goal was to understand better the fundamental mechanisms that underlie bipedal walking in the hopes that this newfound understanding will facilitate better mechanical and control design for bipedal robots. Bipedal walking is hybrid in nature, characterized by periodic contact between a robot and the environment, i.e., the ground. Dynamic models derived from Lagrangians modeling mechanical systems govern the continuous dynamics while discrete dynamics were handed by an impact model using impulse-like forces and balancing angular momentum. This combination of continuous and discrete dynamics motivated the use of hybrid systems for modeling purposes.

The framework of hybrid systems was used to model three-dimensional bipedal walking in a general setup for a robotic model with a hip, knees, and feet with the goal of obtaining stable walking. To achieve three-dimensional walking, functional Routhian reduction was used to decouple the sagittal and coronal dynamics. By doing so, it was possible to achieve walking in the two-dimensional sagittal plane on the three-dimensional model, restricted to operate in the sagittal plane. Imposing this restriction resulted in a reduced-order model, referred to as the sagittally-restricted model. Sagittal control in the form of controlled symmetries and additional control strategies was used to achieve stable walking on the sagittally-restricted model.

Functional Routhian reduction was then applied to the full-order system. The sagittal control developed on the reduced-order model was used with reduction to achieve walking in three dimensions in simulation.

The control schemes described resulted in walking which was remarkably anthropomorphic in nature. This observation is surprising given the simplistic nature of the controllers used. Moreover, the two-dimensional and three-dimensional dynamics were completely decoupled inasmuch as the dynamic models governing the sagittal motion were equivalent. Additionally, the reduction resulted in swaying in the lateral plane. This motion, which is generally present in human walking, was unplanned and was a side-effect of the decoupling process. Despite the approximate nature of the reduction, the motion was still almost completely decoupled with respect to the sagittal and coronal planes.

ACKNOWLEDGMENTS

I would like to acknowledge the National Science Foundation for its generous support of my research through the Graduate Research Fellowship Program. I would also like to acknowledge my advisor, Aaron Ames; his guidance and support were invaluable in achieving my research goals. I would like to thank the other members of my committee, Reza Langari, Richard Malak, and Robin Murphy, for their advice and support which will hopefully carry me through the completion of my dissertation. I would also like to thank Jessy Grizzle at the University of Michigan, Ann Arbor and Christine Chevallereau at Ecole Centrale de Nantes for their help understanding the modeling and control of bipedal robots. Finally, I would like to thank my parents and grandmother. Without them my accomplishments would be long forgotten. I thank my brother and sister who helped keep things in perspective while I was busy with my research.

TABLE OF CONTENTS

CHAPTER Page

LIST OF FIGURES

LIST OF TABLES

CHAPTER I

INTRODUCTION

The concept of bipedal robotic walking has been present in the minds of scientists for as long as the concept of robots. There is something intrinsically fascinating about the idea of a robot that walks like a human which inspires awe in the minds of all, scientists and laymen alike. Many attempts have been made in recent history to achieve bipedal robotic walking—most of these attempts involve some form of control engineering—and yet the majority of walking that has been achieved, either in implementation or in simulation, has displayed statically-stable walking or, at the very least, is a far cry from the walking seen in humans. Indeed, dynamically-stable walking was only first introduced in 1990 by McGeer [1]. This cardinal paper ushered in a new era of research into dynamically-stable robotic walking. Over the next two decades, new research was conducted which resulted in the development of control schemes which allow for dynamically-stable walking in robotic models. Some of the approaches used involve passivity-based control [2, 3], control of zero-moment point [4, 5], hybrid zero dynamics [6–8], central pattern generators [9, 10], compliance-based control [11], and human-inspired feedback control [12, 13].

The objective of this thesis is to show how *anthropomorphic* bipedal walking

---

The journal model is *IEEE Transactions on Automatic Control.*

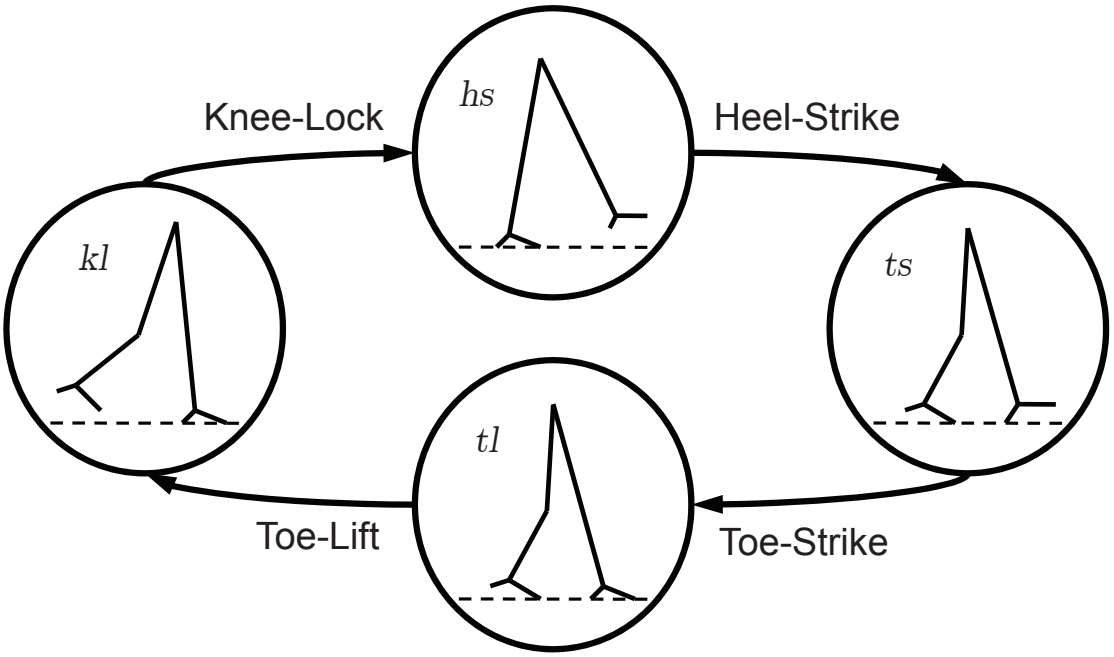

Fig. 1: Directed graph for the hybrid model considered in this thesis.

can be achieved through simulation on a bipedal robot model. In order to achieve truly anthropomorphic walking, it will be necessary to first examine the human gait and isolate those characteristics which define the gait. There is a sizeable body of work studying human walking (see, for example [14–19]) and in the majority of studies, the human gait is broken down into discrete phases—this can be represented mathematically as a directed graph as illustrated by example in Fig. 1. The definition of each phase and the number of phases vary from study to study. For example, in [14], the human gait is broken down into swing and stance phases for each leg, and the swing phase is further broken down into three sub-phases: initial swing, mid swing, and terminal swing.

Traditionally, control of bipedal robots considers a relatively small number of domains; i.e., five domains or less. For example, the compass gait walker which has been studied to exhaustion (see, e.g., [1], or see [20] for a more detailed analysis) has

only a single domain whereas the kneed biped considered in [21] has a gait consisting of two domains and the kneed biped with feet considered in [22] has a gait consisting of five domains. When designing a biped it is important to carefully consider the domains which will comprise the model's graph. Two models with different graphs could require substantial differences in controller design in order to achieve walking. In this thesis, a model will be considered in which the domain breakdown was determined through a subjective analysis of human walking. One literally observes a human walking and tries to ascertain what is happening. Some simplifications, e.g., knee-lock are made to simplify controller design. Indeed, this is the traditional method for designing a hybrid model of a biped. However, recent results show how to create a hybrid model through objective analysis of experimental human walking data [23].

The study of bipedal walking requires research in either robotics and control or biomechanics. In the context of biomechanics, researchers are often interested in forces and dynamics [19, 24]; specifically, forces and loading have been studied at the foot [25, 26] and at the hip [27, 28]. Such analysis is useful in the design of prostheses and hip replacements yet fails to give a complete picture of human walking. While many studies have been conducted in the context of biomechanics [29], few have been done with respect to control engineering [30, 31]. When studying the biomechanics of walking, researchers use force plates and force loading models to measure and estimate the distribution of musculoskeletal forces and ground reaction forces [32]. This is used in conjunction with either inverse-dynamic models [33, 34] or forward-dynamic models [35–37].

Another important concept in the study of bipedal walking is the idea of single support and double support phases. In a single support phase, the system has only a single point or collection of points on a rigid body—for example, a foot can be flat on the ground—on the system in contact with the ground whereas in a double support

phase, the system has multiple points or collections of points on different rigid bodies in contact with the ground—for example, this could mean that the stance foot is in flat contact with the ground and the non-stance foot is rolling about the toe. Double support phases introduce a new level of complexity when modeling the mechanics of bipeds because virtual forces must be imposed to achieve the desired interaction of the model with the ground; these forces are typically referred to as Lagrange multipliers in the literature [38]. Despite the difficulties associated with double support phases, it is still important to consider double support when trying to achieve humanlike walking. Indeed, humans spend an appreciable portion of their walking gaits having double support.

A major concern that arises when designing controllers for bipedal walkers is the physical limitation of the system. Specifically, ground reaction forces must be obeyed before a controller can be implemented on a physical model. As an example, consider a robot with feet. It must be verified that the feet do in fact stay flat and do not roll about an edge. Additionally, it must be verified through impact that specific contact constraints are physically satisfied. For example, if the non-stance heel strikes the ground, one must check the constraint forces to see whether or not the back foot leaves the ground instantaneously. Finally, friction must be considered to ensure that the robot does not slip.

Another problem that arises in bipedal walking is the increase in complexity when trying to achieve walking three dimensions. Two-dimensional walking, i.e., walking in the sagittal plane, is comparatively easy to obtain. Results on three-dimensional walking are limited [21, 39–42] due to the difficulty of the problem. Most research on bipedal robots comes from three major schools of thought:[1] controlled symmetries,

[1]These schools of thought are related to the control of bipedal robots to obtain dynamically-stable walking. There is a wealth of literature on a technique known

hybrid zero dynamics and reduction-based techniques. *Controlled symmetries* [2, 53] is a technique for translating passive walking down varying slopes to controlled walking on flat ground [54]; the greatest shortcoming of this theory is that it requires full actuation. In order to deal with underactuated bipeds, the notion of *hybrid zero dynamics* was introduced [6, 8, 55–57]. This theory creates a lower-dimensional system that captures the behavior of the higher-dimensional system and has been successful in the construction of two two-dimensional bipeds, RABBIT and MABEL (see [58, 59]). The first two techniques predominantly have been applied to two-dimensional bipeds. (Although hybrid zero dynamics has recently been extended to three-dimensional bipedal robots [39–41, 60], this extension is still in its initial stages.)

The desire to have an intuitable and straightforward bridge between two- and three-dimensional walking motivates the introduction of *reduction-based techniques*. Reduction-based techniques will be the main theoretical tool used in this thesis to extend two-dimensional walking to three dimensions. Reduction-based techniques use geometric reduction—in the form of functional Routhian reduction (first introduced in [61])—to decouple the sagittal and coronal dynamics of a biped and have been successfully applied to obtain three-dimensional walking for simpler bipeds than the one considered in this thesis, e.g., [21, 62, 63] (all of which were fully-actuated). The technique used in this paper works as follows:

In the control scheme presented in this paper (cf. [42]), *three* different control laws will be leveraged—energy shaping, functional Routhian reduction, and input/output linearization—along with a set of control laws which gives walking for the *sagittally-*

---

as zero moment point (ZMP) [5, 43–46]. In addition, obtaining dynamically-stable walking without control through minimal mechanical design has also been well-studied [1, 3, 47–51]. Finally, see [52] for a good review on the comparison between the "humanoid" (using ZMP techniques) and "minimalist" (using mechanical design) approach to bipedal robots.

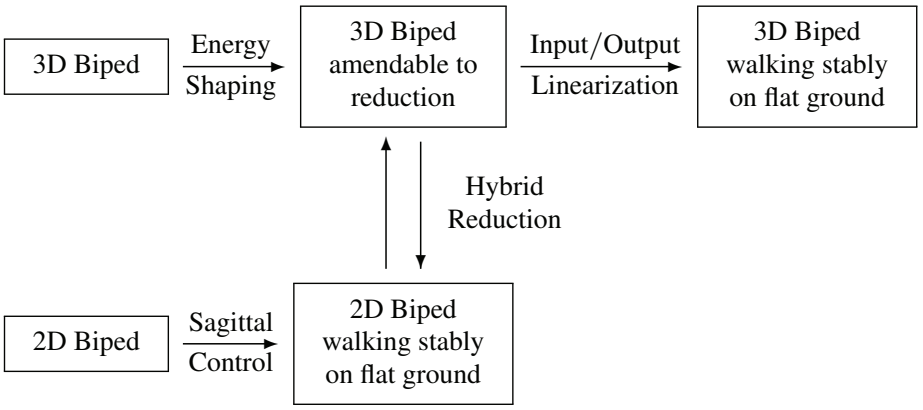

Fig. 2: Overview of reduction control scheme.

restricted biped. (Many different sets of control laws would work for this; however, in this thesis, a set of laws similar to those in [22] will be used.) These control laws will be combined in a novel fashion to obtain a single control law that will be applied on each discrete domain where the biped is fully-actuated as indicated in Fig. 2. More specifically, sagittal control is applied to a two-dimensional biped obtained by restricting the three-dimensional biped to the sagittal plane. The first control law then uses *energy shaping* to transform the Lagrangian modeling the dynamics of the three-dimensional biped; this results in a hybrid system amenable to functional Routhian reduction. The second control law, *functional Routhian reduction*, is then applied to this system—the reduced system obtained by applying this form of geometric reduction is exactly the two-dimensional biped—thus decoupling the sagittal and coronal dynamics while simultaneously stabilizing the coronal dynamics (for certain initial conditions satisfying the Theorem 1 of this thesis). Finally, the third control law, *input/output linearization*, stabilizes to the surface of initial conditions for which the decoupling afforded by the second control law is valid through the use of a virtual output chosen so that, when zero, the proper initial conditions are satisfied.

It is important to understand how the application of the above control laws

is affected by the discrete structure and relationship to the continuous dynamics. Specifically, there are only three discrete domains (of four) in which the biped is fully-actuated (domains *tl*, *kl*, and *hs* in Fig. 1). Yet, the above control scheme requires full actuation and thus can only be used in those three discrete domains. Surprisingly, this is enough since the majority of the gait is spent in these three domains. This illustrates the relationship between the discrete representation and continuous dynamics and the importance of drawing inspiration from human walking.

This thesis starts with a discussion of mechanics and modeling of bipedal robots. Next, the notion of a hybrid system is introduced. These ideas will then be combined to construct the hybrid model of a three-dimensional biped that will be studied in this thesis. This will be followed by a discussion of controller design for the two-dimensional sagittaly-restricted biped and it will be shown how the designed controllers can be to achieve walking gaits; the results of a simulation doing this will be given. Then, functional Routhian reduction will be described and control laws will be given which implement reduction. These control laws will be applied to the three-dimensional biped and simulation results will be given which show three-dimensional walking. The thesis will conclude with a discussion of open problems and potential ideas worthy of future study.

CHAPTER II

MODELING BIPEDAL ROBOTS

Bipedal robots are modeled as kinematic chains. A kinematic chain is essentially a series of rigid bodies connected by joints. Modeling can be done using any of a number of mathematical formalisms ubiquitous in the field of mechanics such as the method of exponential twists [64] or the Denavit-Hartenberg convention [65]. Computation of the dynamics of such a system can be performed many different ways; however, straightforward implementation of the corresponding mathematical formulas generally results in unnecessary computational complexity. It is possible—and, in fact, common practice—to simplify the process of obtaining the system dynamics by using well-known numerical methods such as those found in [66]. Modeling methods are well known and can be found, for example, in [67, 68].

An important aspect of bipedal walking is ground contact. At different points in a walking gait, a biped will have either one point or multiple points in contact with the ground. Because different types of ground contact require different constraints, it will be natural to model different walking phases by the constraints imposed. This will lead to the requirement that hybrid systems be used to model bipedal walking. Hybrid systems combine continuous dynamics—the continuous-time evolution of the state variables that govern the configuration of the system as differential equations—and discrete dynamics—changes in which constraints are being applied to the system (for example, heel-strike). Hybrid systems will be formally defined and discussed in the next chapter. Before formally introducing hybrid systems, however, it will be

convenient to first discuss continuous and discrete dynamics.

This chapter will start by discussing how to model a kinematic chain in a generalized configuration with no constraint assumptions such as ground contact. It will be shown how to calculate the Lagrangian of a robotic model and then how to use the Lagrangian to obtain a dynamic model. After discussing Lagrangian mechanics, a general formalism for constraints will be introduced and then used to deal with the concept of ground contact. It will be shown how to impose constraints and verify the validity of a given constraint taking into consideration ground reaction forces and friction. Combining the mechanics and constraints will give a complete model for the continuous dynamics of a biped. The chapter will end with a discussion of impact dynamics which will constitute the discrete dynamics of a biped.

A. Generalized Model

The generalized robot model which will be considered is an n-link kinematic chain in free space. The model will be developed in three dimensions and later, where appropriate, two-dimensional models will be considered. It will be trivial to obtain the two-dimensional equations given the formulation in three dimensions. The formulation given here will be similar to the one used in [40].

First, consider a robot that is free to move in the world frame. Therefore, let R_0 be the *world frame*—this is an inertial reference frame which is fixed with respected to the environment. Then, let R_b be a reference frame attached to a point on the robot as in Fig. 3.[1] Let $p_b \in \mathbb{R}^3$ represent the Cartesian position of R_b as measured in

[1]There are infinite choices of where to place R_b but some choices of location result in simpler dynamics. In general, the simplest dynamics result when R_b is placed at the center of the hip. The reason that this is simpler than, for instance, the foot is that the forward kinematics of each link of the system is found as the product of rotation matrices. Each additional product substantially increases the complexity of

the world frame R_0 and let $\phi_b \in SO(3)$[2] represent the orientation of R_b as measured with respect to R_0. Next, let $q \in \mathcal{Q} \subseteq \mathbb{R}^n$ be the *shape coordinates*[3] of the system where $\mathcal{Q}$ is the system's *configuration space*. Combining these variables results in a set of coordinate that can model an n-link robot in a generalized configuration:

$$q_e = \begin{bmatrix} p_b \\ \phi_b \\ q \end{bmatrix}. \tag{2.1}$$

For simplicity, define the *generalized configuration space* $\mathcal{Q}_e$ as

$$q_e \in \mathcal{Q}_e = \mathbb{R}^3 \times SO(3) \times \mathcal{Q}. \tag{2.2}$$

This will be useful later as it will define part of the state space for the nonlinear control system modeling the dynamics of the robot.[4]

Now that a proper choice of coordinates has been given, the dynamics can be found using the method of Lagrange (see, for example, [70, pp. 253–260]). The first step is to calculate the Lagrangian of the system. This is easily done using, for example, the method of exponential twists found in [64, pp. 168–169]. The kinetic energy of a mechanical system, $T_e : T\mathcal{Q}_e \to \mathbb{R}$, can be written in the following form:

$$T_e(q_e, \dot{q}_e) = \frac{1}{2} \dot{q_e}^T D_e(q_e)\, \dot{q}_e$$

---

the dynamics. Therefore, placing R_b to minimize the largest number of product terms required to calculate the forward dynamics of the end-effector generally results in the minimal complexity.

[2] $SO(3)$ represents the special orthogonal group in three dimensions and is sometimes called a rotation group. For more on this, see [69].

[3] Sometimes, q will be referred to as the configuration variable as it defines the configuration of the system with respect to the body-fixed frame R_b.

[4] The state space of the system will later be given as $\mathcal{X} = T\mathcal{Q}_e$.

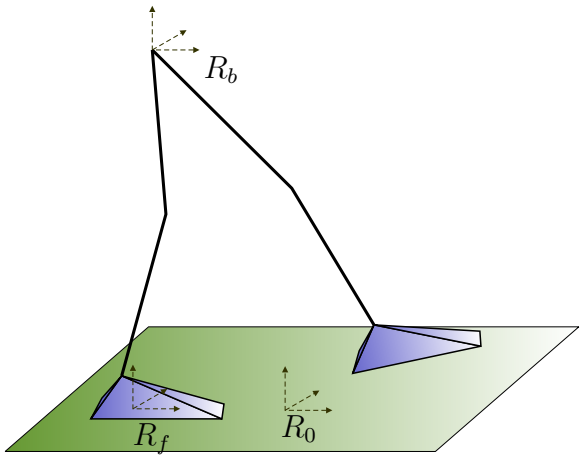

Fig. 3: Robot showing a body frame R_b and a world frame R_0. The body frame is attached to the robot and the world frame is an inertial reference frame. A frame R_f is attached to a foot.

where $D_e : \mathcal{Q}_e \to \mathbb{R}^{n_e \times n_e}$ is the *manipulator inertia matrix* with $n_e = \dim \mathcal{Q}_e = 6 + n$ and the potential energy, $V_e : \mathcal{Q}_e \to \mathbb{R}$, is written $V_e(q_e)$. The potential energy will be a result of gravity and, if present, mechanical springs. Combining the kinetic energy and the potential energy results in the Lagrangian $L_e : T\mathcal{Q}_e \to \mathbb{R}$ given by

$$L_e(q_e, \dot{q}_e) = T_e(q_e, \dot{q}_e) - V_e(q_e). \tag{2.3}$$

Using the above Lagrangian (2.3), the dynamics of the robot can be calculated using the Euler-Lagrange equation (see [71]):

$$\mathcal{EL}_{q_e}(L_e) \triangleq \frac{d}{dt}\frac{\partial L_e}{\partial \dot{q}_e}(q_e, \dot{q}_e) - \frac{\partial L_e}{\partial q_e}(q_e) = B_e(q_e)u(q_e, \dot{q}_e) + \Upsilon_{nc}(q_e, \dot{q}_e) \tag{2.4}$$

where $B_e : q_e \to \mathbb{R}^{n_e \times n_e}$ is a torque distribution matrix which is constant for the proper choice of coordinates, $u(q_e, \dot{q}_e)$ represents state feedback control and $\Upsilon_{nc}(q_e, \dot{q}_e)$ represents nonconservative forces other than control. Without loss of generality, these

force terms will sometimes be grouped as

$$\Upsilon(q_e, \dot{q}_e) = B_e(q_e)u(q_e, \dot{q}_e) + \Upsilon_{nc}(q_e, \dot{q}_e) \tag{2.5}$$

such that $\Upsilon : T\mathcal{Q}_e \to \mathbb{R}^n_e$ represents all nonconservative forces acting on the system, e.g. viscous dampers or control (see [72, pp. 34–45]). Following the procedure in [64, pp. 171], (2.4) for a robot can be written

$$D_e(q_e)\,\ddot{q}_e + C_e(q_e, \dot{q}_e)\,\dot{q}_e + G_e(q_e) = \Upsilon(q_e, \dot{q}_e) \tag{2.6}$$

where $C_e : T\mathcal{Q}_e \to \mathbb{R}^{n_e \times n_e}$ contains Coriolis terms and centrifugal terms and $G_e : \mathcal{Q}_e \to \mathbb{R}^{n_e}$, which is given by

$$G_e(q_e) = \frac{\partial V_e}{\partial q_e}(q_e), \tag{2.7}$$

contains terms resulting from the potential energy, i.e., gravitational forces and spring forces. For convenience, the dynamic model can be written as a control system (f_e, g_e) where

$$\begin{aligned} f_e(q_e, \dot{q}_e) &= \begin{bmatrix} \dot{q}_e \\ D_e^{-1}(q_e)\left(-C_e(q_e, \dot{q}_e)\,\dot{q}_e - G_e(q_e) + \Upsilon_{nc}(q_e, \dot{q}_e)\right) \end{bmatrix}, \\ g_e(q_e) &= \begin{bmatrix} \mathbf{0}_{n\times m} \\ D_e^{-1}(q_e)B_e(q_e) \end{bmatrix} \end{aligned} \tag{2.8}$$

are the vector and control fields, respectively. In (2.8), $B_e(q_e)$ is a torque distribution matrix as in (2.4) and (2.5).

B. Constraints

As mentioned previously, a central feature of bipedal locomotion is ground contact. In the previous section, a model for a robot in a generalized position was given. This

model is free to translate and rotate in space. To properly achieve bipedal walking, it will be necessary to impose constraints on the dynamics of the system in order to keep points on one foot or both feet in contact with the ground. In general, a bipedal robot can have two types of support: *single support* and *double support*. Single support is categorized by those domains of the gait in which only one foot is in contact with the ground while double support represents those domains in which both feet are in contact with the ground simultaneously. Both single support and double support can be achieved by imposing constraints on (2.6). Imposing constraints acts to constrain the operational space of the system to be on some restricted submanifold. This fact will be used later to define a domain of admissibility for the system.

Two types of constraints will be defined in this section: holonomic constraints and unilateral constraints.[5] Holonomic constraints will be constraints that physically restrict the motion of a system. For this reason, holonomic constraints are sometimes called kinematic constraints as they provide restrictions on the kinematics of a system. Holonomic constraints have a number of uses[6] but, in this paper, they will be used to enforce ground contact and knee-lock. Unilateral constraints will be used to parameterize the distance to impact of, for instance, the heel of the non-stance foot of a robot. It will become clear soon how unilateral constraints are used to derive the impact dynamics of the system. Unilateral constraints will not restrict the kinematics of a system however they will restrict the operational range of the system; i.e., the robot is not permitted to go below the ground. Holonomic constraints will affect both the continuous and discrete dynamics of a system whereas unilateral constraints will only affect the discrete dynamics (i.e., the impact equations).

[5]See [40] for more information on both types of constraints

[6]Some examples of this can be found in [21, 22].

1. Holonomic Constraints

Holonomic constraints will be considered first as they provide actual constraints on the kinematics of the system. Consider the following definition of a holonomic constraint:

Definition 1. *A holonomic constraint is defined to be a tuple* $\boldsymbol{\eta} = (\mathcal{Q}, L, \eta)$*, where*

- $\mathcal{Q}$ *is the configuration space,*
- $L : T\mathcal{Q} \to \mathbb{R}$ *is a hyperregular Lagrangian with* $q \in \mathcal{Q}$*,*
- $\eta : T\mathcal{Q} \to \mathbb{R}^c$ *provides* c *holonomic constraints on the configuration space; we assume that the zero level sets of the constraints,* $\eta_i^{-1}(0) \forall i \in [1, c]$*, are smooth manifolds.*

A holonomic constraint provides an implicit constraint on the system (see [73]); that is, a holonomic constraint cannot be written in explicit form and must instead be written as an implict equation of the form:

$$\eta(q, \dot{q}) = \text{constant}.$$

Consider the holonomic constraint $\boldsymbol{\eta} = (\mathcal{Q}, L, \eta)$ with $q \in \mathcal{Q}$ as given in (2.1) and (2.2) and L as given in (2.3). This tuple represents a holonomic constraint[7] on the robot's configuration space $\mathcal{Q}$. The actual constraint, $\eta(q, \dot{q})$, when imposed on the system, will satisfy the following equation:

$$\eta(q, \dot{q}) = J(q)\, \dot{q} = \text{constant}. \tag{2.9}$$

It is important to note that $J(q)$ should have full rank; that is, $\operatorname{rank} J(q) = c$ where

[7]The actual equation of the constraint $\eta(q, \dot{q})$ contained in the tuple $\boldsymbol{\eta}$ can be a vector containing multiple constraints. At the risk of introducing ambiguity, a holonomic constraint will be considered to be a single equation as the constraints are written in vector form.

$c = \dim \eta(q, \dot{q})$. The matrix $J(q)$ is commonly called a Jacobian matrix.

In general, a holonomic constraint of dimension c, when imposed on the dynamic model of the system, will act to restrict the tangent bundle of the system's configuration space. The result will be that the system operates on a codimension-c embedded submanifold. According to the principle of virtual work found in [64, 74–76], there exists a *wrench*[8] F containing forces and/or torques that, when applied to the system, will cause (2.9) to be satisfied provided that $J(q)$ has full rank. This wrench is imposed on the system by augmenting the dynamic model (2.6) as follows:

$$D(q)\dot{q} + C(q, \dot{q})\dot{q} + G(q) = \Upsilon(q, \dot{q}) + J^T(q)F(q, \dot{q}). \tag{2.10}$$

The expression for $F(q, \dot{q})$ can be found by combining (2.9) and (2.10). Differentiating (2.9) gives

$$\dot{J}(q, \dot{q})\,\dot{q} + J(q)\,\ddot{q} = 0. \tag{2.11}$$

Premultiplying (2.10) by $D^{-1}(q)$ and rearranging terms gives

$$\ddot{q} = D^{-1}(q)\left(\Upsilon(q, \dot{q}) + J^T(q)F(q, \dot{q}) - C(q, \dot{q})\dot{q} - G(q)\right). \tag{2.12}$$

Substitution of (2.12) into (2.11) yields

$$\dot{J}(q, \dot{q})\,\dot{q} + J(q)D^{-1}(q)\left(\Upsilon(q, \dot{q}) + J^T(q)F(q, \dot{q}) - C(q, \dot{q})\dot{q} - G(q)\right) = 0. \tag{2.13}$$

Rearranging terms from (2.13) gives

$$\begin{aligned} J(q)D^{-1}(q)J^T(q)F(q, \dot{q}) = \\ -\dot{J}(q, \dot{q})\,\dot{q} + J(q)D^{-1}(q)\left(\Upsilon(q, \dot{q}) - C(q, \dot{q})\dot{q} - G(q)\right). \end{aligned} \tag{2.14}$$

[8] See [77] for more on wrenches.

Finally, premultiplying by $(J(q)D^{-1}(q)J^T(q))^{-1}$ gives the desired expression for the wrench $F(q,\dot{q})$ which imposes the kinematic constraint (2.9):

$$F(q,\dot{q}) = -\left(J(q)D^{-1}(q)J^T(q)\right)^{-1}\cdot \left(\dot{J}(q,\dot{q})\dot{q} + J(q)D^{-1}(q)\left(\Upsilon(q,\dot{q}) - C(q,\dot{q})\dot{q} - G(q)\right)\right). \tag{2.15}$$

Thus, the force $F(q,\dot{q})$ from (2.15) has limitations of the form:

$$F(q,\dot{q}) < 0.$$

For example, for a system with friction coefficient μ, horizontal force F_h, and vertical force F_v, to avoid linear slipping requires that the following constraint be satisfied (see [78, pp. 132]):

$$|F_h| < \mu F_v$$

where F_v is assumed to be oriented in the direction of gravity. Combining (2.10) and (2.15) leads to the following vector and control fields:

$$f(q,\dot{q}) = \begin{bmatrix} \dot{q} \\ \mathcal{D}^{-1}(q)\Big((I - J^T(q)\Xi(q)A(q)\mathcal{D}^{-1}(q))\cdot \\ \qquad (\Upsilon_{nc}(q,\dot{q}) - \mathcal{C}(q,\dot{q})\dot{q} - \mathcal{G}(q)) - J^T(q)\Xi(q)\dot{J}(q)\dot{q}\Big) \end{bmatrix},$$

$$g(q) = \begin{bmatrix} \mathbf{0}_{(n\times m)} \\ \mathcal{D}^{-1}(q)\left(I - J^T(q)\Xi(q)J(q)\mathcal{D}^{-1}(q)\right)B(q) \end{bmatrix}, \tag{2.16}$$

with $\Xi(q)$ defined as

$$\Xi(q) := \left(J(q)\mathcal{D}^{-1}(q)J^T(q)\right)^{-1}. \tag{2.17}$$

These results will soon be used to model ground contact, but, first, a discussion

of unilateral constraints is pertinent.

2. Unilateral Constraints

Unilateral constraints are constraints which are not physically imposed on a system. Instead, they are used, in the case of bipedal robots, to parameterize the distance to impact of an end-effector. Consider, for example, the unilateral constraint shown in Fig. 4. In this case, the unilateral constraint is the height of the non-stance heel above the ground. When this height reaches zero, an impact will occur and it will be time to transition to the next domain (or phase) of the walking gait. It is therefore easy to to see how unilateral constraints can be used to obtain *guards* or *switching surfaces*. Consider the following formal definition of a unilateral constraint:

Definition 2. *A unilateral constraint is defined to be a tuple* $\mathbf{h} = (\mathcal{Q}, L, h(q))$*, where*

- $\mathcal{Q}$ *is the configuration space,*
- $L : T\mathcal{Q} \to \mathbb{R}$ *is a hyperregular Lagrangian with* $q \in \mathcal{Q}$*,*
- $h : \mathcal{Q} \to \mathbb{R}$ *provides a unilateral constraint on the configuration space; we assume that the zero level set of the constraint,* $h^{-1}(0)$*, is a smooth manifold.*

As mentioned previously, a unilateral constraint can naturally lead to a guard for a given domain on a hybrid system. Due to the hybrid nature of the guard, this discussion will be deferred until the next chapter. Having introduced both holonomic and unilateral constraints, it is now possible to introduce the domain of admissibility.

C. Domain of Admissibility

As can be seen in the previous section, holonomic and unilateral constraints introduce restrictions on the configuration space of the system. In other words, the system will

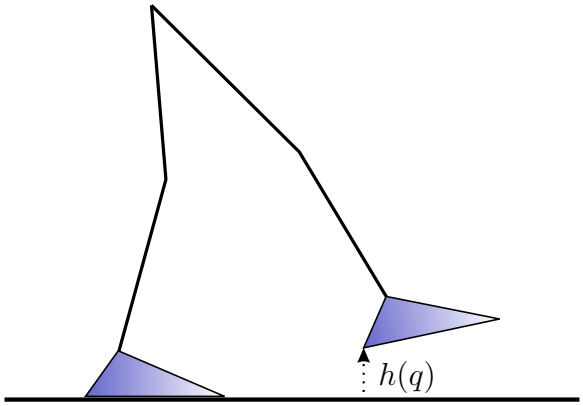

Fig. 4: Example of a unilateral constraint, $h(q)$. This example constraint parameterizes the height of the non-stance heel above the ground.

be required to operate on a restricted submanifold called the *domain of admissibility*. Mathematically, the domain of admissibility, $\mathcal{D}$, is a submanifold of the tangent bundle of a configuration space; i.e., for a given configuration space, $\mathcal{Q}$, it holds that $\mathcal{D} \subseteq T\mathcal{Q}$.

Consider a system with Lagrangian L and configuration variable $q \in \mathcal{Q}$. Then assume this system is constrained with *domain restriction vector* $\mathcal{H}(q, \dot{q}, u)$ satisfying

$$\mathcal{H}(q, \dot{q}, u) < 0.$$

This can result from a combination of holonomic constraints and/or a unilateral constraint as will be seen in the following sections. The domain restriction vector acts to confine the system to operate on the space of the domain where $\mathcal{H}(q, \dot{q}, u) < 0$; this leads to the following definition for *domain of admissibility*:

Definition 3. *Given a configuration space $\mathcal{Q}$ and a domain restriction vector $\mathcal{H}(q, \dot{q}, u)$, the domain of admissibility of a system is given by*

$$\mathcal{D} = \left\{ \begin{bmatrix} q^T & \dot{q}^T & u^T \end{bmatrix}^T \in T\mathcal{Q} \times \mathbb{R}^m : \mathcal{H}(q, \dot{q}, u) > 0 \right\} \tag{2.18}$$

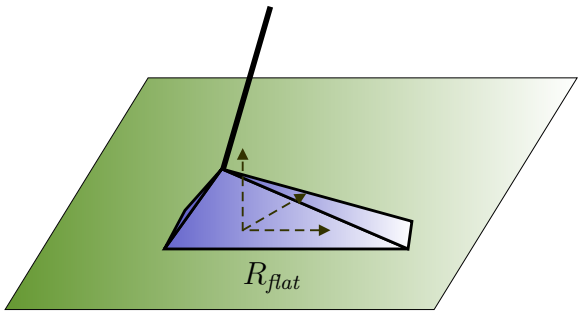

Fig. 5: An example of a robot with flat foot ground contact. A reference frame, R_{flat}, is attached to a flat foot.

with m the number of control inputs.

In order for the assumptions of walking to be valid, the system must operate within the domain of admissibility on any given domain. It will be shown in the next sections how to apply this concept to the system of interest.

D. Ground Contact

Holonomic constraints, as discussed in the previous section, will be the tool of choice for dealing with ground contact. The dynamic model for such a system will be of the form given in (2.10) and the *ground contact wrench* that will maintain ground contact will be of the form (2.15). In order to properly model ground contact, it will be necessary to consider a system with generalized configuration space $\mathcal{Q}_e$. This section will now consider the different types of ground contact which can occur in the various phases composing the walking gait of a bipedal robot.

1. Flat Foot Contact

In order to achieve humanlike bipedal locomotion, it is required that the feet of the robot do not slip. In other words, the friction between the feet and the floor must

be sufficient to avoid slipping. For the case of a foot in flat contact with the ground as in Fig. 5, a holonomic constraint will be used to prevent the foot from moving. To begin, attach a reference frame R_{flat} to the flat foot as in Fig. 5 and let ${}^{flat}T_0(q_e)$ be a (4×4) homogeneous transformation matrix which represents a transformation between the world frame R_0 and the flat foot frame R_{flat}. According to [79, pp. 329], the velocity transformation matrix ${}^{flat}_{0}\mathbf{\Omega}_{flat}(q_e, \dot{q}_e)$[9] is given by

$$\begin{aligned} {}^{flat}_{0}\mathbf{\Omega}_{flat}(q_e, \dot{q}_e) &= {}^{flat}T_0^T(q_e)\ {}^{flat}\dot{T}_0(q_e, \dot{q}_e) \\ &= \begin{bmatrix} {}^{flat}_{0}\boldsymbol{\omega}_{flat}(q_e, \dot{q}_e) & {}^{flat}\mathbf{v}_{flat}(q_e, \dot{q}_e) \\ \mathbf{0}_{1\times 3} & 0 \end{bmatrix} \end{aligned} \tag{2.19}$$

where ${}^{flat}\mathbf{v}_{flat}(q_e, \dot{q}_e)$ is the linear velocity of the origin of R_{flat} with respect to R_0 expressed in R_{flat} and ${}^{flat}_{0}\boldsymbol{\omega}_{flat}(q_e, \dot{q}_e)$ is a skew-symmetric matrix (see [80]) containing the angular velocity of R_{flat} with respect to R_0 expressed in R_{flat}. The angular velocities can be found from the following equation (cf. [79, pp. 298]):

$${}^{flat}_{0}\boldsymbol{\omega}_{flat}(q_e, \dot{q}_e) = \begin{bmatrix} 0 & -\omega_z(q_e, \dot{q}_e) & \omega_y(q_e, \dot{q}_e) \\ \omega_z(q_e, \dot{q}_e) & 0 & -\omega_x(q_e, \dot{q}_e) \\ -\omega_y(q_e, \dot{q}_e) & \omega_x(q_e, \dot{q}_e) & 0 \end{bmatrix} \tag{2.20}$$

For convenience, group the angular velocities into a vector:

$${}^{flat}\boldsymbol{\omega}_{flat}(q_e, \dot{q}_e) = \begin{bmatrix} \omega_x(q_e, \dot{q}_e) \\ \omega_y(q_e, \dot{q}_e) \\ \omega_z(q_e, \dot{q}_e) \end{bmatrix}. \tag{2.21}$$

[9] ${}^{flat}_{0}\mathbf{\Omega}_{flat}$ expresses the body velocity of the flat foot's frame R_{flat} with respect to the world frame R_0 in the flat foot's frame R_{flat}.

Using equations (2.19), (2.20), and (2.21), the holonomic constraint necessary to achieve flat foot contact can be expressed as

$$\eta_{flat}(q_e, \dot{q}_e) = J_{flat}(q_e)\,\dot{q}_e = \begin{bmatrix} {}^{flat}\mathbf{v}_{flat}(q_e, \dot{q}_e) \\ {}^{flat}\boldsymbol{\omega}_{flat}(q_e, \dot{q}_e) \end{bmatrix} = \mathbf{0}_{6\times 1}. \tag{2.22}$$

Requiring that the linear and angular velocities of the foot be zero effectively fixes the foot on the ground. This holonomic constraint can be imposed on the dynamic model (2.10) using the wrench $F_{flat}(q_e, \dot{q}_e)$, which can be calculated using (2.15) with the kinematic constraint given in (2.22), which is expressed in the frame R_{flat}. The first three components of $F_{flat}(q_e, \dot{q}_e)$ are the ground reaction forces and the last three components are the ground reaction torques:

$$F_{flat}(q_e, \dot{q}_e, u) = (F^{fx}_{flat}, F^{fy}_{flat}, F^{fz}_{flat}, F^{mx}_{flat}, F^{my}_{flat}, F^{mz}_{flat})^T, \tag{2.23}$$

where the dependence of each element on $q_e, \dot{q}_e$ has been suppressed.

In general, the constraining ground reaction wrench will have limitations. There is no limitation on the normal force in the positive direction, but to avoid take-off, it is necessary that

$$F^{fz}_{flat}(q_e, \dot{q}_e, u) > 0. \tag{2.24}$$

The force of friction exerted by the ground on the foot has limitations on its magnitude. If the force becomes to great, the robot will slip. This leads to the constraint

$$\sqrt{\left(F^{fx}_{flat}(q_e, \dot{q}_e)\right)^2 + \left(F^{fy}_{flat}(q_e, \dot{q}_e)\right)^2} < \mu F^{fz}_{flat}(q_e, \dot{q}_e),$$

where μ is the coefficient of static friction. This represents a friction cone which is nonlinear; to use linear constraints, this can be replaced with a friction pyramid which

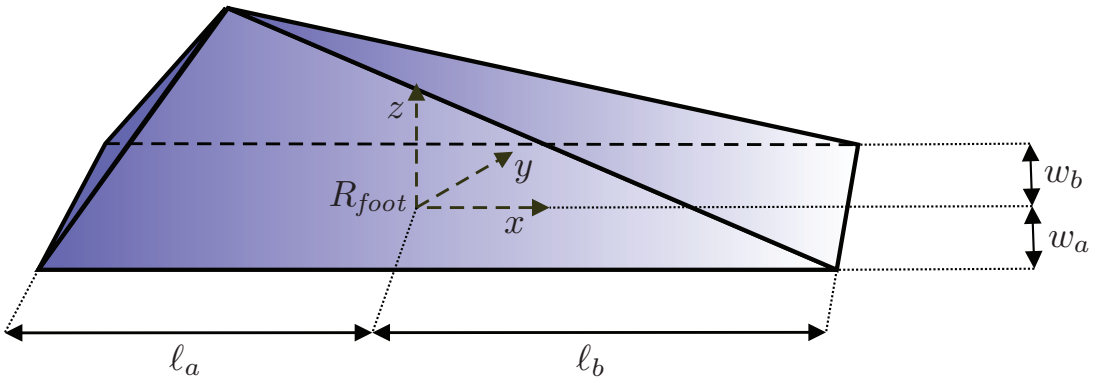

Fig. 6: The dimensions of robot foot. These measurements specify lengths from the origin of the foot-fixed frame R_{foot} to the edges.

gives a conservative approximation:

$$|F^{fx}_{flat}(q_e, \dot{q}_e, u)| < \frac{\mu}{\sqrt{2}} F^{fz}_{flat}(q_e, \dot{q}_e, u), \tag{2.25}$$

$$|F^{fy}_{flat}(q_e, \dot{q}_e, u)| < \frac{\mu}{\sqrt{2}} F^{fz}_{flat}(q_e, \dot{q}_e, u). \tag{2.26}$$

Additionally, the ground reaction torque preventing the foot from rotating up onto an edge is limited by (see [81, 82]):

$$-w_b F^{fz}_{flat}(q_e, \dot{q}_e, u) < F^{mx}_{flat}(q_e, \dot{q}_e, u) < w_a F^{fz}_{flat}(q_e, \dot{q}_e, u), \tag{2.27}$$

$$-\ell_a F^{fz}_{flat}(q_e, \dot{q}_e, u) < F^{my}_{flat}(q_e, \dot{q}_e, u) < \ell_b F^{fz}_{flat}(q_e, \dot{q}_e, u), \tag{2.28}$$

where w_a, w_b, ℓ_a, ℓ_b are as shown in Fig. 6. In the literature, (2.25) is called the *Zero Moment Point (ZMP)* (see [44, 46]).

The constraints (2.24), (2.25), (2.27), (2.28) must all be satisfied for the walking to be physically realizable. Because the equations are linear inequalities, they can be grouped into the domain restriction vector

$$\mathcal{H}_{flat}(q_e, \dot{q}_e, u) := A^T_{F_{flat}}(q_e) F_{flat}(q_e, \dot{q}_e, u) > 0. \tag{2.29}$$

Note the dependence on the applied torque, u. Using Definition 3, the domain of admissibility is as in (2.18):

$$\mathcal{D}_{flat} = \left\{ \begin{bmatrix} q_e^T & \dot{q_e}^T & u^T \end{bmatrix}^T \in T\mathcal{Q}_e \times \mathbb{R}^m : \mathcal{H}_{flat}(q_e, \dot{q_e}, u) > 0 \right\} \tag{2.30}$$

Satisfying these constraints can be extremely difficult. The most difficult constraints to meet are (2.27) and (2.28) and there are a variety of control schemes which achieve walking by doing so; see [43, 83]. In this thesis, it is assumed that the foot is sufficiently wide and long to satisfy and that friction is sufficiently large; however, it is checked that (2.24) is satisfied

2. Rolling Contact

At times in a bipedal gait, the ground contact is not always confined to have a flat foot. Sometimes, the foot is rotating about an edge. For example, when a human walks, he typically lands on his heel and his foot rolls forward until it is flat. Similarly, the heel of the back foot generally leaves the ground before the toe. See [15] for pictures of human walking. In dealing with rolling contact, it is assumed that the contact occurs at either the toe edge of the heel edge and therefore occurs about the y-axis.

As in the treatment of flat foot contact, attach a reference frame R_{roll} to a foot as in Fig. 5. The y-axes of the reference frame and the axis of rotatin must be colocated; that is, the y-axis of R_{roll} must be lined up with the toe or heel edge. Let ${}^{roll}T_0(q_e)$ be a (4×4) homogeneous transformation matrix which represents a transformation between the world frame R_0 and the foot frame R_{roll}. As before, let ${}^{roll}\mathbf{v}_{roll}(q_e, \dot{q_e})$ be the linear velocity of the origin of R_{roll} with respect to R_0 expressed in R_{roll} and ${}^{roll}\boldsymbol{\omega}_{roll}(q_e, \dot{q_e})$ be the body-fixed angular velocity vector for R_{roll}.

Using ${}^{roll}\mathbf{v}_{roll}(q_e, \dot{q_e})$ and ${}^{roll}\boldsymbol{\omega}_{roll}(q_e, \dot{q_e})$, the holonomic constraint necessary to

achieve rolling foot contact can be expressed as

$$\eta_{roll}(q_e, \dot{q}_e) = J_{roll}(q_e)\,\dot{q}_e = \begin{bmatrix} {}^{roll}\mathbf{v}_{roll}(q_e, \dot{q}_e) \\ \omega_x(q_e, \dot{q}_e) \\ \omega_z(q_e, \dot{q}_e) \end{bmatrix} = \mathbf{0}_{6\times 1}. \tag{2.31}$$

It can be seen that (2.31) is similar to the flat foot case (2.22). The one difference is that (2.31) does not have $\omega_y(q_e, \dot{q}_e)$. Removing this entry from (2.22) allows for rotation about the y-axis; i.e., the foot can roll about the heel or toe.

This holonomic constraint can be imposed on the dynamic model (2.10) using the wrench $F_{roll}(q_e, \dot{q}_e)$, which can be calculated using (2.15) with the kinematic constraint given in (2.31), which is expressed in the frame R_{roll}. The first three components of $F_{roll}(q_e, \dot{q}_e)$ are the ground reaction forces and the last two components are the ground reaction torques:

$$F_{roll}(q_e, \dot{q}_e) = \begin{bmatrix} F_{roll}^{fx} & F_{roll}^{fy} & F_{roll}^{fz} & F_{roll}^{mx} & F_{roll}^{mz} \end{bmatrix}^T \tag{2.32}$$

where the dependence of each element on $q_e, \dot{q}_e$ has been suppressed.

As in the case of flat foot contact, there exist restrictions on ground reactions forces and torques; specifically, equations (2.24), (2.25), and (2.27) are applicable here as follows

$$F_{roll}^{fz} > 0. \tag{2.33}$$

$$|F_{roll}^{fx}| < \frac{\mu}{\sqrt{2}} F_{roll}^{fz}, \tag{2.34}$$

$$|F_{roll}^{fy}| < \frac{\mu}{\sqrt{2}} F_{roll}^{fz}. \tag{2.35}$$

$$-w_b F_{roll}^{fz} < F_{roll}^{mx} < w_a F_{roll}^{fz}, \tag{2.36}$$

where w_a, w_b are as shown in Fig. 6 and μ is the coefficient of static friction. As

before, these constraints can be written linearly as $A_{F_{roll}}(q_e)F_{roll}(q_e, \dot{q_e}, u)$ and can be expressed as a domain restriction vector:

$$\mathcal{H}_{roll}(q_e, \dot{q_e}, u) = A^T_{F_{roll}}(q_e)F_{roll}(q_e, \dot{q_e}, u) > 0.$$

Using this vector the domain of admissbility is as given in (2.18):

$$\mathcal{D}_{roll} = \left\{ \begin{bmatrix} q_e^T & \dot{q_e}^T & u^T \end{bmatrix}^T \in T\mathcal{Q}_e \times \mathbb{R}^m : \mathcal{H}_{roll}(q_e, \dot{q_e}, u) > 0 \right\} \tag{2.37}$$

E. Knee-Lock

When making kneed bipeds walk, it greatly simplies the problem to introduce periods of the gait where the knee is locked. Landing on a locked knee prevents the biped from crumpling over upon heel-strike. This type of contact can be implemented physically using a lock or clutch system. In modeling the biped, the locked knee is treated with a holonomic constraint. The necessary constraint for the choice of coordinates considered in this thesis is simple. Let ϑ_{knee} represent a knee angle. In the models considered, this will be ϑ_2 or ϑ_5. Locking the stance and non-stance knee can therefore be expressed as kinematic constraints:

$$\eta^{stk}_{lock}(q_e, \dot{q_e}) = J^{stk}_{lock}(q_e)\,\dot{q_e} = \dot{\vartheta}_2, \tag{2.38}$$

$$\eta^{nsk}_{lock}(q_e, \dot{q_e}) = J^{nsk}_{lock}(q_e)\,\dot{q_e} = \dot{\vartheta}_5. \tag{2.39}$$

The above constraints (2.38) and (2.39) will lock the stance and non-stance knees, respectively. Assuming the knees lock in the zero position leads to restrictions on the system viz.

$$\mathcal{H}^{stk}_{lock}(q_e, \dot{q_e}) = (\vartheta_2, \dot{\vartheta}_2)^T,$$

$$\mathcal{H}^{nsk}_{lock}(q_e, \dot{q_e}) = (\vartheta_5, \dot{\vartheta}_5)^T,$$

which lead to the following domains of admissibility as given in (2.18):

$$\mathcal{D}^{stk}_{lock} = \left\{ \begin{bmatrix} q_e^T & \dot{q_e}^T & u^T \end{bmatrix}^T \in T\mathcal{Q}_e \times \mathbb{R}^m : \mathcal{H}^{stk}_{lock}(q_e, \dot{q_e}) = 0 \right\}, \tag{2.40}$$

$$\mathcal{D}^{nsk}_{lock} = \left\{ \begin{bmatrix} q_e^T & \dot{q_e}^T & u^T \end{bmatrix}^T \in T\mathcal{Q}_e \times \mathbb{R}^m : \mathcal{H}^{nsk}_{lock}(q_e, \dot{q_e}) = 0 \right\}. \tag{2.41}$$

These domains of admissbility mean that the corresponding knee angle is reduced from the system entirely and a reduced model can be used that does not include this angle if desired. Furthermore, there are no restrictions on the strength of the lock.

F. Combining Constraints

There will be times in the gait when more than one of the previously described constraints will be required. The most interesting example of this is the case of double support—for this, it would be necessary to constrain both feet to the ground in some combination of flat contact and rolling contact. Another example which applies for the continuous dynamics of every domain is knee-lock. This is applied on one or both knees in every domain and must be applied alongside the constraints on foot contact.

Double support is an important component of the human gait. Indeed, an appreciable portion of the gait is spent in double support (see [84]). Much of the literature is concerned with instantaneous double support phases. This thesis, however, considers double support through the continuous dynamics of some parts of the gait.

Combining constraints is relatively straightforward. First, consider c holonomic constraints on a system, $\boldsymbol{\eta}_1 = (\mathcal{Q}, L, \eta_1(q, \dot{q}), \ldots, \boldsymbol{\eta}_c(q) = (\mathcal{Q}, L, \eta_c(q, \dot{q}))$. Following the procedure for flat foot contact and rolling contact, let $J_1(q), \cdots, J_c(q)$ be Jacobian

matrices satisfying

$$\eta_1(q, \dot{q}) = J_1^T(q)\, \dot{q} = \mathbf{0},$$
$$\cdots,$$
$$\eta_c(q, \dot{q}) = J_c^T(q)\, \dot{q} = \mathbf{0}$$

where $\mathbf{0}$ is the zero matrix of appropriate dimension in each case. Now, the constraints can be combined to have Jacobian

$$J(q) = \text{Basis}\left(\text{RowSp}\left(\begin{bmatrix} J_1^T(q) & \cdots & J_c^T(q). \end{bmatrix}^T\right)\right)$$

Now assume that each of the above constraints has a domain restriction vector, $\mathcal{H}_1(q, \dot{q}, u), \ldots, \mathcal{H}_c(q, \dot{q}, u)$, where the vector can possibly be of zero dimension; this occurs for knee-lock where any restraining force is admissible. These domain restriction vectors can be combined viz.

$$\mathcal{H}(q, \dot{q}, u) = \left(\mathcal{H}_1^T(q, \dot{q}, u), \ldots, \mathcal{H}_c^T(q, \dot{q}, u)\right)^T.$$

which results in the domain of admissibility

$$\mathcal{D} = \mathcal{D}_1 \cap \cdots \cap \mathcal{D}_c$$

with $\mathcal{D}_1, \ldots, \mathcal{D}_2$ the domains of admissibility given the associated constraints.

G. Model Reduction

The model of interest in this thesis has a discrete graph composed of four domains. In each of these domains, different holonomic constraints are imposed to achieve the desired ground contact and knee-lock behaviors. To simplify computation, model reduction can be used on each domain, removing constrained coordinates. For example,

if the knee is locked, it is not necessary to consider the knee angle as a variable since it is constant through the domain. Such a trick is common in the literature [21, 22]. By reducing the number of coordinates, we can simulate the system more quickly.

H. Impact Model

Impacts occur throughout the gait at various points as a function of gait design. A impact occurs when a point, line, or surface comes into contact with the ground. The contact is assumed to be rigid and plastic. In the hybrid model considered in this thesis, there are three impacts that occur during one step: toe-strike, knee-lock, and heel-strike. The mechanics is involved but can be found in, for example, [85, 86]. For robotic manipulators, the mechanics of has been addressed for tool use in [87, 88].

Various different types of impact models have been considered. For example, one model assumes an elastic impact and model deformation of rigid bodies as in [56, 89]. While this type of model provides a more accurate description of the impact than does a rigid model, many of the necessary parameter must be estimated and so the accuracy of such a model is questionable.

The impacts considered in this thesis follow the rigid impact model developed by [90]. Such an impact results in an instantaneous change in velocity as a result of conservation of angular momentum; angular positions, however, remain unchanged. Therefore, let q_e^- and q_e^+ represent the velocities right before and right after impact, respectively, and let t^- and t^+ represent the times corresponding to these velocities. Then introduce an impulsive force vector $\delta_{F_{imp}}$ which acts on a system during impact via the dynamic model:

$$D_e(q_e)\,\ddot{q}_e + C_e(q_e,\dot{q}_e)\,\dot{q}_e + G_e(q_e) = B_e(q_e)u(q_e,\dot{q}_e) + J^T(q_e)\delta_{F_{imp}}(q_e,\dot{q}_e).$$

Integrating this model under the assumption that the actuators do not produce impulsive torques yields:

$$D_e(q_e)(\dot{q_e}^+ - \dot{q_e}^-) = J^T(q_e)F_{imp}(q_e, \dot{q_e}) \tag{2.42}$$

where

$$F_{imp} = \int_{t^-}^{t^+} \delta_{F_{imp}}\left(q_e(\tau), \dot{q_e}(\tau)\right)\, d\tau.$$

For this system, $J^T(q_e)F_{imp}(q_e, \dot{q_e})$ is a measure of angular momentum. Specifically, the equation (2.42) represents conservation of angular momentum through impact. In order to determine how the forces are applied, it is necessary to determine the value of the Jacobian matrix $J(q_e)$. The procedure for this is the same as in the continuous case. Assume that the impact is to be constrained with holonomic constraint $\boldsymbol{\eta} = (\mathcal{Q}_e, L_e, \eta(q_e, \dot{q_e}))$. Then, the appropriate $J(q_e)$ satisfies

$$\eta(q_e, \dot{q_e}) = J(q_e)\,\dot{q_e} = 0. \tag{2.43}$$

Imposing such a constraint will ensure that, after impact, the constraints are satisfied; for example, the foot is flat on the ground and not moving. Combining (2.42) and (2.43) results in the following impact model:

$$\begin{bmatrix} D_e(q_e) & -J^T(q_e) \\ J(q_e) & \mathbf{0} \end{bmatrix} \begin{bmatrix} \dot{q_e}^+ \\ F_{imp}(q_e, \dot{q_e}) \end{bmatrix} = \begin{bmatrix} D_e(q_e)\,\dot{q_e}^- \\ \mathbf{0} \end{bmatrix} \tag{2.44}$$

where $\mathbf{0}$ represents the zero matrix of appropriate size. The model (2.44) can be used to calculate post-impact velocities using conservation of angular momentum. Using the Schur complement (c.f. [91]), it is possible to give an expression for the

post-impact velocity map $P : \mathcal{G}_e \to \mathcal{D}_e$ as

$$P(q_e) = \left(I - D_e^{-1}(q_e) J^T(q_e) \left(J(q_e) D_e^{-1}(q_e) J^T(q_e) \right)^{-1} J(q_e) \right) \dot{q}_e. \tag{2.45}$$

This map takes a point $(q_e, \dot{q}_e) \in \mathcal{G}_e$ on the guard and maps it back to the domain of the system. Using the expression (2.45) eliminates the impulsive force F_{imp}; however, when checking the assumptions on a gate, it is necessary to see if the impulsive forces in F_{imp} are physically reasonable; that is, does the system belong to the domain of admissibility. These must be checked in the same manner as in the continuous case. Therefore, the reader is referred to the previous sections on flat foot and rolling contact; specifically, the domains of admissibility for these types of contact were given in (2.30) and (2.37), respectively. The general definition of domain of admissbility was given in Definition 3; see (2.18).

Remark 1. *It is important to note that the impact model is only valid if the resulting state belongs to the domain of admissibility. For example, if that a constraint will be imposed after impact, but this assumption turns out to be false based on the forces in F_{imp}, then the impact model must be recomputed removing the constraint which was violated.*

One last important point is leg switching. In order to take advantage of the natural symmetry of walking, a variable can be introduced representing which leg is the stance leg. The end result will be a biperiodic gait. Swapping the legs is done on the transition from *hs* to *ts* using a relabeling matrix $\mathcal{R}(q_e)$. Using the relabeling matrix and the post-impact velocity map, it is possible to give an expression for the reset map:

$$\Delta(q_e, \dot{q}_e) = \begin{bmatrix} \mathcal{R}(q_e)\, q_e \\ \mathcal{R}(q_e)\, P(q_e, \dot{q}_e) \end{bmatrix} \tag{2.46}$$

Remark 2. *Depending on the model and the conditions impact, an interesting phenomenon can occur in whihc the foot bounces slightly and rebounds an infinite number of times over a finite time interval. Such a phenomenon is refered to in the literature as the Zeno phenomenon; see [92–95]. In general, this behavior is not desireable and should be avoided through control design.*

CHAPTER III

HYBRID SYSTEMS

In this chapter, we define the notion of a hybrid system and describe how it can be constructed to model a physical system. In order to model hybrid systems, we must first formally define hybrid systems. *Hybrid systems* or *systems with impulse effects* [8] are dynamical systems which consist of both continuous dynamics—a differential equation representing the continuous motion of a mechanical system as a function of time—and discrete dynamics—mechanical impacts resulting from contact with the environment or the system itself which result in discrete (instantaneous) changes in the velocity variable of a system.

A. Formal Definition of Hybrid Systems

Consider the following definition of a hybrid system:

Definition 4. *A hybrid system is a tuple*

$$\mathscr{H} = (\Gamma, \mathcal{D}, \mathcal{G}, \Delta, \mathcal{F}),$$

where

- $\Gamma = (V, E)$ *is an oriented or directed graph, i.e., V and E are each a set of vertices and edges, respectively, and there exists a source function* $\mathrm{sor} : E \to V$ *and a target function* $\mathrm{tar} : E \to V$ *which associate to an edge its source and target, respectively.*

- $\mathcal{D} = \{\mathcal{D}_v\}_{v \in V}$ *is a set of domains, where* $D_v \subseteq \mathbb{R}^n$ *is a smooth submanifold of* $\mathbb{R}^n$,
- $\mathcal{G} = \{\mathcal{G}_e\}_{e \in E}$ *is a set of guards, where* $G_e \subseteq \mathcal{D}_{\mathrm{sor}(e)}$,
- $\Delta = \{\Delta_e\}_{e \in E}$ *is a set of reset maps, where each* $\Delta_e : \mathcal{G}_e \to \mathcal{D}_{\mathrm{tar}(e)}$ *is a smooth map,*
- $\mathcal{F} = \{f_v\}_{v \in E}$, *where* f_v *is a dynamical system on* $\mathcal{D}_v$, *i.e.,* $\dot{x} = f_v(x)$ *for* $x \in \mathcal{D}_v$.

A hybrid system can be used to model various mechnical system which consist of both continuous and discrete dynamics such as a bouncing ball. Such a systems has one domain and is called a *simple hybrid system* as shown in Fig. 7. It can be seen that the reset map carries the trajectory back to the same domain. It can be seen that this definition does not allow for control. In the case of bipedal walking, it will be necessary to have some type of control. This motivates the following definition of a *hybrid control system*:

Definition 5. *A hybrid control system is a tuple*

$$\mathscr{HC} = (\Gamma, \mathcal{D}, \mathcal{U}, \mathcal{G}, \Delta, \mathcal{FG}),$$

where

- $\Gamma = (V, E)$ *is an oriented or directed graph, i.e., V and E are each a set of vertices and edges, respectively, and there exists a source function* $\mathrm{sor} : E \to V$ *and a target function* $\mathrm{tar} : E \to V$ *which associate to an edge its source and target, respectively.*
- $\mathcal{D} = \{\mathcal{D}_v\}_{v \in V}$ *is a set of domains, where* $D_v \subseteq \mathbb{R}^n$ *is a smooth submanifold of* $\mathbb{R}^n$,

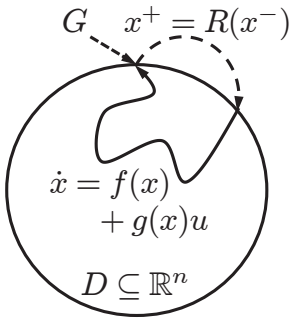

Fig. 7: Graphical interpretation of a simple hybrid system.

- $\mathcal{U} = \{\mathcal{U}_v\}_{v \in V}$ *is a set of admissible controls (in this paper, assumed to be equivalent to* $\mathbb{R}^m$*),*
- $\mathcal{G} = \{\mathcal{G}_e\}_{e \in E}$ *is a set of guards, where* $G_e \subseteq \mathcal{D}_{\mathrm{sor}(e)}$*,*
- $\Delta = \{\Delta_e\}_{e \in E}$ *is a set of reset maps, where each* $\Delta_e : \mathcal{G}_e \to \mathcal{D}_{\mathrm{tar}(e)}$ *is a smooth map,*
- $\mathcal{FG} = \{(f_v, g_v)\}_{v \in E}$*, where* (f_v, g_v) *is a control system on* $(\mathcal{D}_v, \mathcal{U}_v)$*, i.e.,* $\dot{x} = f_v(x) + g_v(x)u$ *for* $x \in \mathcal{D}_v$ *and* $u \in \mathcal{G}_v$*.*

A hybrid system is simply a hybrid control system with $\mathcal{U} = \{0\}$, in which case $F = \{f_v\}$ with $\dot{x} = f_v(x)$.

B. Poincaré Map

Solutions to hybrid systems, or hybrid flows or hybrid executions, are defined in the traditional manner (see [96]). A solution to a hybrid system is k-periodic if it returns to the same point after passing through the domain in which it is contained k times. (In the process it may pass through an arbitrary number of other domains of the hybrid system.) One can consider the local exponential stability of k-periodic solutions in the obvious way (see [63] for this definition in the case of a hybrid system with one

domain). One can associate to a k-periodic solution of a hybrid system a Poincaré map, and the stability of the k-periodic solution can be determined by considering the stability of the Poincaré map. Finally, stability can be determined numerically using approximations of the Jacobian of the Poincaré map (see [57, 97]). This method will be used to determine that the periodic orbits for the models considered in this paper are stable.

CHAPTER IV

BIPEDAL MODELS

Recall that the overarching goal of this thesis is to obtain walking on a three-dimensional bipedal model. In order to achieve humanlike walking, it is necessary to have a humanlike model. Therefore, this thesis considers a biped having knees and feet. Adding knees to a biped is important not only because humans have knees but because knees allow the biped to achieve ground clearance for the swing foot. Adding feet is even more important because it allows a biped to have full actuation for at least part of the gait—in other words, there will be one degree of acuation for each degree of freedom. In the case of bipeds, this means that a robot will have actuation at the ankle. As will later be shown in simulation, much of the sagittal motion is a result of actuation on the stance ankle. Additionally feet will allow for lateral stabilization of the biped (see [21, 42, 48]).

Before describing the model considered, it will be helpful to define the concept of *full actuation* and *underactuation*. Following the definition, illustrative example will be given.

Definition 6. *Let m represent the number of control inputs to a system and let n represent a choice of general coordinates on the system. The coordinates of the system must chosen such that the number of coordinates give the minimal representation; i.e., there are no redundant coordinates. Then: A system is said to be fully-actuated or to have full actuation if the number of control inputs, m, is equal to the number of degrees of freedom of the system, n, that is $m = n$, or to be underactuated or to have*

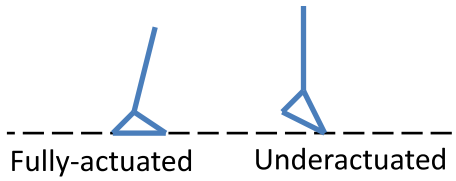

Fig. 8: Different types of actuation.

underactuation if the number of control inputs, m, is less than the number of degrees of freedom of the system, n, that is, $m < n$.

Example 1. *Fig. 8 shows the difference between full actuation and underactuation. For underactuation, one can see that there is an additional angle between the foot and the ground that is not present in the fully-actuated biped, yet there is no additional actuator. How can one connect a motor between the foot and the floor? This lack of actuation is one of the fundamental challenges encountered when designed point-footed robots and is an important reason for considering feet.*

Now that the difference between underactuation and full actuation has been made clear, it is possible to describe the bipedal models of interest in this thesis. To be clear, a three-dimensional model is considered as well as a sagittaly-restricted version of this model. Due to space constraints and the complexity of the expressions, the specific equations for the Lagrangians and constraint functions used to define the systems are not included but can be found online at [98].

The models will be defined as follows: first, the three-dimensional model will be described completely. Then, a sagittal restriction will be applied to the three-dimensional model which will result in a reduced, two-dimensional model.

Consider the following hybrid control system which will define the three-dimensional

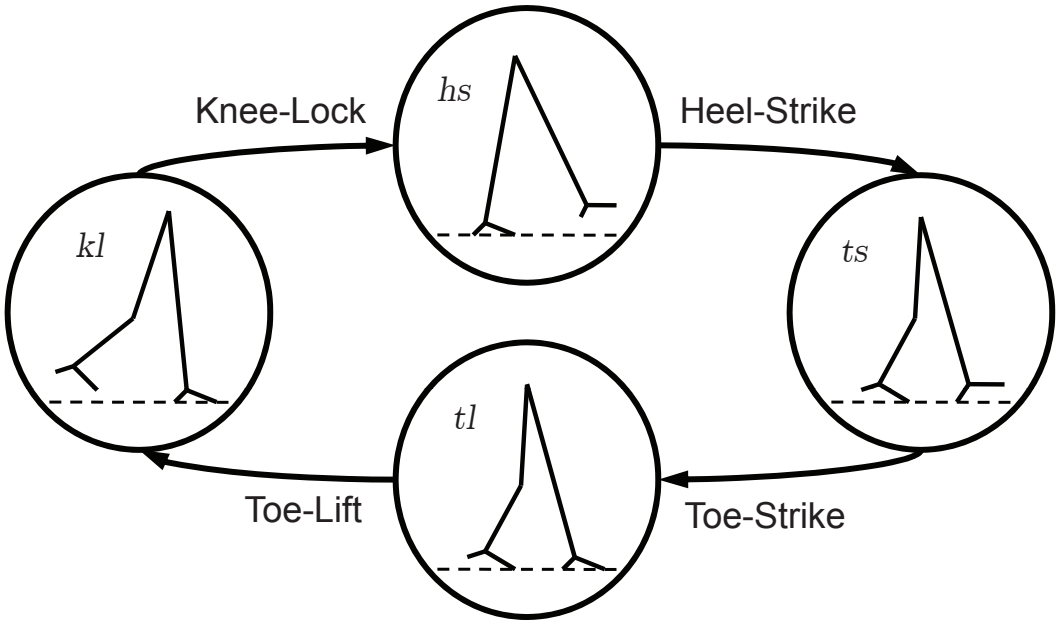

Fig. 9: Domain graph, Γ, of the hybrid model the biped.

bipedal model:

$$\mathscr{HC}_{3D} = (\Gamma_{3D}, \mathcal{D}_{3D}, \mathcal{U}_{3D}, \{\mathcal{G}_{3D,i}\}, \{\Delta^i_{3D}\}, \{\mathcal{FG}_{3D,i}\}) \tag{4.1}$$

for $i \in \{ts, tl, kl, hs\}$ with the elements in (4.1) as defined in Definition 5. The elements of this tuple will be given in the remainder of this section which will fully define the hybrid control system for the three-dimensional model.

A. Discrete Structure

The model considered has discrete structure—with four states in a loop with a specific temporal order—defined by the oriented graph Γ_{3D}, given by

$$\Gamma_{3D} = \big(\{ts, tl, kl, hs\}, \{e_{ts} = (ts, tl), e_{tl} = (tl, kl), e_{kl} = (kl, hs), e_{hs} = (hs, ts)\}\big).$$

A visual representation of the discrete structure can be seen in Fig. 9.

B. Mechanical Configuration

The bipedal model has feet and locking knees. Both feet and locking knees will require the use of holonomic constraints. Which constraints are enforced on each domain will be described shortly. The mechanical configuration is governed by the generalized coordinates

$$q_e = (p_x, p_y, p_z, \phi_x, \phi_y, \phi_z, \vartheta, \varphi) \in \mathbb{R}^3 \times \mathbb{T}^3 \times S \times \mathbb{T}^2 = \mathcal{Q}_e,$$

where the shape space S has coordinates

$$(\vartheta_1, \vartheta_2, \vartheta_3, \vartheta_4, \vartheta_5, \vartheta_6) \in S$$

and $\varphi = (\varphi_1, \varphi_2)$.

The admissible control on all domains will be $\mathcal{U}_{3\mathrm{D}} = \mathbb{R}^8$; however, on domains with locked knees, it will not be helpful to apply actuation to the locked knees, so no control will be applied to a knee when it is locked.

The physical configuration of the biped is given in Fig. 10. This mechanical model has Lagrangian

$$L_e(q_e, \dot{q_e}) = \frac{1}{2}\dot{q_e}^T D_e(q_e)\dot{q_e} - V_e(q_e) \tag{4.2}$$

which can be used to derive the dynamic model of the system. The maps $D_e : \mathcal{Q}_e \to \mathbb{R}^{n \times n}$ and $V_e(q_e) : \mathcal{Q}_e \to \mathbb{R}$ represent the inertia matrix and potential energy of the biped, respectively, and can be found using the standard methods [64]. The dynamic model for a given domain will depend on which holonomic constraints are enforced in that domain.

The model considered has a hip and moves in three-dimensions to the extent allowed by the angles of the system. Specifically, the biped can fall over on its side

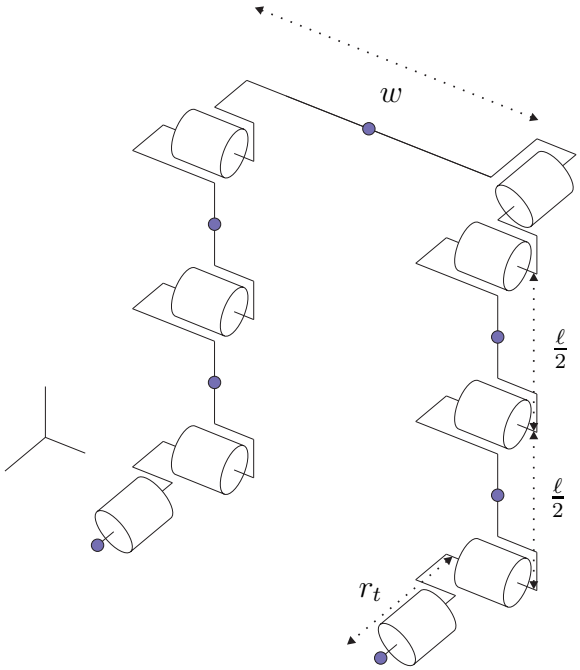

Fig. 10: Physical model of biped. Body coordinates $q_{3\mathrm{D}}$ and physical parameters of the biped are shown.

by rolling laterally (i.e., rotation in the coronal plane). Incidentally, this problem will be taken care of by the reduction scheme used in this thesis. Additionally, as will be mentioned later, when appropriate, reduction will make use of a sagittal restriction—this essentially removes the coronal angles from the system by setting them to zero. This fact will be used later when designing control laws which give two-dimensional walking in the sagittal plane.

The four domains in the hybrid model will now be considered, one at a time, and the rest of the elements of (4.1) will be given. These remaining elements will potentially be different on each domain, depending on the constraints on the system.

1. Domain 1 (ts)

The non-stance knee is unlocked and the system is rotating about the stance heel, i.e., there is rolling contact as in Section II-D-2. Furthermore, the stance knee is locked and the non-stance toe is fixed in place on the ground. These two conditions motivate holonomic constraints to model the system.

a. Constrained Dynamics

The constraint vector will combine the kinematic constraints for rolling contact on both the stance heel and non-stance toe with a kinematic constraint for knee lock of the stance knee into the following holonomic constraint

$$\boldsymbol{\eta}_{\mathrm{3D},ts} = (\mathcal{Q}_e, L_e, \eta_{\mathrm{3D},ts})$$

where the vector constraint $\eta_{\mathrm{3D},ts}(q_{\mathrm{3D}}, \dot{q}_{\mathrm{3D}})$ on the kinematics of the system is

$$\begin{bmatrix} \eta^{sth}_{roll}(q_e, \dot{q}_e) \\ \eta^{nsh}_{flat}(q_e, \dot{q}_e) \\ \eta^{stk}_{lock}(q_e, \dot{q}_e) \end{bmatrix} = \eta_{\mathrm{3D},ts}(q_e, \dot{q}_e) = J_{\mathrm{3D},ts}(q_e)\, \dot{q}_e \tag{4.3}$$

where $\eta^{sth}_{roll}(q_e, \dot{q}_e)$ and $\eta^{nsh}_{roll}(q_e, \dot{q}_e)$ are given in (2.31) with reference frames aligned with the stance heel and non-stance toe, respectively, and $\eta^{stk}_{lock}(q_e, \dot{q}_e)$ is as given in (2.38). Using the constraint (4.3), the dynamic model is given by (2.10) with Jacobian matrix $J_{ts}(q_e)$ satisfying $J_{ts}(q_e)\, \dot{q}_e = \eta_{\mathrm{3D},ts}(q_e, \dot{q}_e)$ and $F_{\mathrm{3D}}(q_e, \dot{q}_e, u)$ the constraint force given

by (2.15). The corresponding control system is then $\mathcal{FG}_{3\mathrm{D},ts} = (f_{3\mathrm{D},ts}, g_{3\mathrm{D},ts})$ where

$$f_{3\mathrm{D},ts}(q_e, \dot{q}_e) = \begin{bmatrix} \dot{q}_e \\ \mathcal{D}_e^{-1}(q_e)\Big((I - J_{ts}^T(q_e)\Xi(q_e)J_{ts}(q_e)\mathcal{D}_e^{-1}(q_e)) \cdot \\ \quad (\Upsilon_{nc}(q_e, \dot{q}_e) - \mathcal{C}_e(q_e, \dot{q}_e)\dot{q}_e - \mathcal{G}_e(q_e)) - J_{ts}^T(q_e)\Xi(q_e)\dot{J}_{ts}(q_e)\dot{q}_e \Big) \end{bmatrix},$$

$$g_{3\mathrm{D},ts}(q_e) = \begin{bmatrix} \mathbf{0}_{(n\times m)} \\ \mathcal{D}_e^{-1}(q_e)\left(I_n - J_{ts}^T(q_e)\Xi(q_e)J_{ts}(q_e)\mathcal{D}_e^{-1}(q_e)\right) B_e(q_e) \end{bmatrix}, \tag{4.4}$$

with $\Xi(q_e)$ as in (2.17).

The guard for this domain is toe-strike which occurs when the stance toe rolls into the ground. This is realized as the unilateral constraint

$$\mathbf{h}_{3\mathrm{D},ts} = (\mathcal{Q}_e, L_e, \eta_{3\mathrm{D},ts}) \tag{4.5}$$

with $h_{3\mathrm{D},ts} : \mathcal{Q}_e \to \mathbb{R}_0^+$ a scalar, representing the height of the stance toe above the ground.

The constraints (4.3) and (4.5) can be combined to obtain a domain restriction vector:

$$\mathcal{H}_{3\mathrm{D},ts}(q_e, \dot{q}_e, u) = \begin{bmatrix} \mathcal{H}_{roll}^{sth}(q_e, \dot{q}_e, u) \\ \mathcal{H}_{roll}^{nsk}(q_e, \dot{q}_e, u) \\ h_{3\mathrm{D},ts}(q_e) \end{bmatrix}$$

where $\mathcal{H}_{roll}^{sth}(q_e, \dot{q}_e, u)$ and $\mathcal{H}_{roll}^{nsk}(q_e, \dot{q}_e, u)$ are as given in (2.31) and $h_{3\mathrm{D},ts}(q_e)$ is as in (4.5). This vector leads to the domain of admissibility

$$\mathcal{D}_{3\mathrm{D},ts} = \left\{ (q_e^T, \dot{q}_e{}^T, u^T)^T \in T\mathcal{Q}_e \times \mathbb{R}^{m_{3\mathrm{D}}} : \mathcal{H}_{3\mathrm{D},ts}(q_e, \dot{q}_e, u) > 0 \right\}$$

and the guard

$$\mathcal{G}_{3\mathrm{D},ts} = \Big\{ (q_e^T, \dot{q}_e{}^T, u^T)^T \in T\mathcal{Q}_e \times \mathbb{R}^{m_{3\mathrm{D}}} : h_{3\mathrm{D},ts}(q_e) = 0 \\ \text{and } \frac{\partial h_{3\mathrm{D},ts}(q_e)}{\partial q_e}\frac{dq_e}{dt} < 0 \Big\}$$

b. Reset Map

As mentioned previously, the transition to the next domain is toe-strike. For this impact, it is desired that, after impact, the stance foot be in flat contact with the ground, that the non-stance toe stays fixed on the ground through impact and that the stance knee stays locked. This suggests the use of a holonomic constraint for flat foot contact as in (2.22) as well as a holonomic constaint for rolling contact on the non-stance foot given by (2.31) and the constraint for knee lock of the stance knee given in (2.38). Combining the associated Jacobian matrices gives the necessary constraint:

$$J_{3\mathrm{D}}^{ts\to tl}(q_e) = \begin{bmatrix} J_{flat}^{stt}(q_e) \\ J_{roll}^{nst}(q_e) \\ J_{lock}^{stk}(q_e) \end{bmatrix}. \tag{4.6}$$

Using the holonomic constraint whose Jacobian matrix is given in (4.6) and the impact model (2.44) results in the reset map $\Delta_{3\mathrm{D}}^{ts\to tl} : T\mathcal{Q}_e \to T\mathcal{Q}_e$ given in (2.46). The relabeling matrix $\mathcal{R}$ is simply the identity matrix; in other words, no relabeling occurs.

2. Domain 2 (tl)

The non-stance knee is unlocked and there is flat foot contact of the stance foot. Furthermore, the stance knee is locked and the non-stance toe is fixed in place on the ground. These conditions introduce holonomic constraints on the system.

a. Constrained Dynamics

The constraint vector will combine the kinematic constraint for flat foot contact on the stance foot with a kinematic constraint for rolling contact on the non-stance toe and a kinematic constraint for locking of the stance knee into the following holonomic constraint

$$\boldsymbol{\eta}_{3\mathrm{D},tl} = (\mathcal{Q}_e, L_e, \eta_{3\mathrm{D},ts})$$

where the constraint vector $\boldsymbol{\eta}_{3\mathrm{D},tl}$ on the kinematics of the system is

$$\eta_{3\mathrm{D},tl}(q_{3\mathrm{D}}, \dot{q}_{3\mathrm{D}}) = \begin{bmatrix} \eta^{sth}_{flat}(q_{3\mathrm{D}}, \dot{q}_{3\mathrm{D}}, u_{3\mathrm{D}}) \\ \eta^{nst}_{roll}(q_{3\mathrm{D}}, \dot{q}_{3\mathrm{D}}, u_{3\mathrm{D}}) \\ \eta^{stk}_{lock}(q_{3\mathrm{D}}, \dot{q}_{3\mathrm{D}}, u_{3\mathrm{D}}) \end{bmatrix} \tag{4.7}$$

with $\eta^{sth}_{flat}(q_e, \dot{q}_e)$ and $\eta^{nsh}_{roll}(q_e, \dot{q}_e)$ given in (2.22) and (2.31), respectively, and having reference frames aligned with the stance heel[1] and non-stance toe, respectively, and $\eta^{stk}_{lock}(q_e, \dot{q}_e)$ as given in (2.38). Using the constraint (4.7), the dynamic model is given by (2.10) with $J(q_e)$ the Jacobian matrix satisfying $J(q_e)\,\dot{q}_e = \eta_{3\mathrm{D},tl}(q_e, \dot{q}_e)$ and $F_{3\mathrm{D}}(q_e, \dot{q}_e, u)$ the constraint force given by (2.15). The corresponding control system

[1]This frame can be attached to any point on the stance foot since the foot is not moving or rotating.

is then $\mathcal{FG}_{3\mathrm{D},tl} = (f_{3\mathrm{D},tl}, g_{3\mathrm{D},tl})$ where

$$f_{3\mathrm{D},tl}(q_e, \dot{q}_e) = \begin{bmatrix} \dot{q}_e \\ \mathcal{D}_e^{-1}(q_e)\Big((I - J_{tl}^T(q_e)\Xi(q_e)J_{tl}(q_e)\mathcal{D}_e^{-1}(q_e)) \cdot \\ \qquad (\Upsilon_{nc}(q_e, \dot{q}_e) - \mathcal{C}_e(q_e, \dot{q}_e)\dot{q}_e - \mathcal{G}_e(q_e)) - J_{tl}^T(q_e)\Xi(q_e)\dot{J}_{tl}(q_e)\dot{q}_e \Big) \end{bmatrix},$$

$$g_{3\mathrm{D},tl}(q_e) = \begin{bmatrix} \mathbf{0}_{(n\times m)} \\ \mathcal{D}_e^{-1}(q_e)\left(I_n - J_{tl}^T(q_e)\Xi(q_e)J_{tl}(q_e)\mathcal{D}_e^{-1}(q_e)\right) B_e(q_e) \end{bmatrix}, \tag{4.8}$$

with $\Xi(q_e)$ as in (2.17).

The constraints (4.7) can be used to write the domain restriction vector,

$$\mathcal{H}_{3\mathrm{D},tl}(q_{3\mathrm{D}}, \dot{q}_{3\mathrm{D}}, u_{3\mathrm{D}}) = \begin{bmatrix} \mathcal{H}_{flat}^{sth}(q_{3\mathrm{D}}, \dot{q}_{3\mathrm{D}}, u_{3\mathrm{D}}) \\ \mathcal{H}_{roll}^{nsk}(q_{3\mathrm{D}}, \dot{q}_{3\mathrm{D}}, u_{3\mathrm{D}}) \end{bmatrix},$$

which leads to the domain of admissibility

$$\mathcal{D}_{3\mathrm{D},tl} = \left\{ (q_{3\mathrm{D}}^T, \dot{q}_{3\mathrm{D}}^T, u_{3\mathrm{D}}^T)^T \in T\mathcal{Q}_e \times \mathbb{R}^{m_{3\mathrm{D}}} : \mathcal{H}_{3\mathrm{D},tl}(q_{3\mathrm{D}}, \dot{q}_{3\mathrm{D}}, u_{3\mathrm{D}}) > 0 \right\}.$$

b. Reset Map

The transition to the next domain is toe-lift. This will naturally occur when the normal force on the non-stance toe goes to zero from the positive side; a positive normal force corresponds to the the force applied by the ground to prevent the toe from falling through the ground. This motivates the following guard:

$$\mathcal{G}_{3\mathrm{D},tl} = \Big\{ (q_{3\mathrm{D}}^T, \dot{q}_{3\mathrm{D}}^T, u_{3\mathrm{D}}^T)^T \in T\mathcal{Q}_e \times \mathbb{R}^{m_{3\mathrm{D}}} : \left(F_{roll}^{nst}(q_{3\mathrm{D}}, \dot{q}_{3\mathrm{D}}, u_{3\mathrm{D}})\right)^{fz} = 0 \\ \text{and } \mathcal{L}_{f_{3\mathrm{D},tl}} \left(F_{roll}^{nst}(q_{3\mathrm{D}}, \dot{q}_{3\mathrm{D}}, u_{3\mathrm{D}})\right)^{fz} < 0 \Big\}$$

where $F_{roll}^{nst}(q_{3\mathrm{D}}, \dot{q}_{3\mathrm{D}}, u_{3\mathrm{D}})$ is as given in (2.32) and $\mathcal{L}_{f_{3\mathrm{D},tl}} \left(F_{roll}^{nst}(q_{3\mathrm{D}}, \dot{q}_{3\mathrm{D}}, u_{3\mathrm{D}})\right)^{fz}$ is a Lie derivative. Note that in $u_{3\mathrm{D}}$ is feedback control and is properly written $u_{3\mathrm{D}}(q_{3\mathrm{D}}, \dot{q}_{3\mathrm{D}})$.

In this transition, there is no impact and so the reset map is simply the identity map $\Delta^{ts}_{3\mathrm{D}} : T\mathcal{Q}_e \to T\mathcal{Q}_e$ given by $R(q_{3\mathrm{D}}, \dot{q}_{3\mathrm{D}}) = (q^T_{3\mathrm{D}}, \dot{q}^T_{3\mathrm{D}})^T$.

3. Domain 3 (kl)

The non-stance knee is unlocked and there is flat foot contact of the stance foot. Furthermore, the stance knee is locked. These conditions introduce holonomic constraints on the system.

a. Constrained Dynamics

The constraint vector will combine the kinematic constraint for flat foot contact on the stance foot with a kinematic constraint for knee lock on the stance knee into the following constraint vector:

$$\boldsymbol{\eta}_{3\mathrm{D},kl} = (\mathcal{Q}_e, L_e, \eta_{3\mathrm{D},kl}).$$

The constraint vector $\eta_{3\mathrm{D},kl}(q_{3\mathrm{D}}, \dot{q}_{3\mathrm{D}})$ on the kinematics of the system is

$$\eta_{3\mathrm{D},kl}(q_{3\mathrm{D}}, \dot{q}_{3\mathrm{D}}, u_{3\mathrm{D}}) = \begin{bmatrix} \eta^{sth}_{flat}(q_{3\mathrm{D}}, \dot{q}_{3\mathrm{D}}, u_{3\mathrm{D}}) \\ \eta^{stk}_{lock}(q_{3\mathrm{D}}, \dot{q}_{3\mathrm{D}}, u_{3\mathrm{D}}) \end{bmatrix} \tag{4.9}$$

with $\eta^{sth}_{flat}(q_e, \dot{q}_e)$ given in (2.22) having reference frame fixed to the stance foot and η^{stk}_{lock} as given in (2.38). Using the constraint (4.9), the dynamic model is given by (2.10) with $J_{3\mathrm{D},kl}(q_e)$ the Jacobian matrix satisfying $J_{3\mathrm{D},kl}(q_e)\,\dot{q}_e = \eta_{3\mathrm{D},kl}(q_{3\mathrm{D}}, \dot{q}_{3\mathrm{D}})$ and constraint force $F_{3\mathrm{D}}(q_{3\mathrm{D}}, \dot{q}_e, u)$ given in (2.15). The corresponding control system is

then $\mathcal{FG}_{3\mathrm{D},kl} = (f_{3\mathrm{D},kl}, g_{3\mathrm{D},kl})$ where

$$f_{3\mathrm{D},kl}(q_e, \dot{q}_e) = \begin{bmatrix} \dot{q}_e \\ \mathcal{D}_e^{-1}(q_e)\Big((I - J_{3\mathrm{D},kl}^T(q_e)\Xi(q_e)J_{3\mathrm{D},kl}(q_e)\mathcal{D}_e^{-1}(q_e)) \cdot \\ (\Upsilon_{nc}(q_e,\dot{q}_e) - \mathcal{C}_e(q_e,\dot{q}_e)\dot{q}_e - \mathcal{G}_e(q_e)) - J_{3\mathrm{D},kl}^T(q_e)\Xi(q_e)\dot{J}_{3\mathrm{D},kl}(q_e,\dot{q}_e)\dot{q}_e \Big) \end{bmatrix},$$

$$g_{3\mathrm{D},kl}(q_e) = \begin{bmatrix} \mathbf{0}_{(n\times m)} \\ \mathcal{D}_e^{-1}(q_e)\left(I_n - J_{3\mathrm{D},kl}^T(q_e)\Xi(q_e)J_{3\mathrm{D},kl}(q_e)\mathcal{D}_e^{-1}(q_e)\right) B_e(q_e) \end{bmatrix}, \qquad (4.10)$$

with $\Xi(q_e)$ as in (2.17).

The guard for this domain is knee-lock which occurs when the non-stance knee swings to an angle of zero and locks. This is realized as the unilateral constraint

$$\mathbf{h}_{3\mathrm{D},kl} = (\mathcal{Q}_e, L_e, \eta_{3\mathrm{D},kl}) \qquad (4.11)$$

with $h_{3\mathrm{D},kl} : \mathcal{Q}_e \to \mathbb{R}_0^+$ a scalar, representing the angle of the non-stance knee. Specifically, $h_{3\mathrm{D},kl}(q_{3\mathrm{D}}) = \vartheta_5$.

The constraints (4.9) and (4.11) can be combined to obtain the domain restriction vector

$$\mathcal{H}_{3\mathrm{D},kl}(q_{3\mathrm{D}}, \dot{q}_{3\mathrm{D}}, u_{3\mathrm{D}}) = \begin{bmatrix} A_{F_{flat}}^T(q_{3\mathrm{D}})F_{flat}(q_{3\mathrm{D}}, \dot{q}_{3\mathrm{D}}, u_{3\mathrm{D}}) \\ h_{3\mathrm{D},kl}(q_{3\mathrm{D}}) \end{bmatrix}$$

This leads to the domain of admissibility

$$\mathcal{D}_{3\mathrm{D},kl} = \left\{ (q_{3\mathrm{D}}^T, \dot{q}_{3\mathrm{D}}^T, u_{3\mathrm{D}}^T)^T \in T\mathcal{Q}_e \times \mathbb{R}^{m_{3\mathrm{D}}} : \mathcal{H}_{3\mathrm{D},kl}(q_{3\mathrm{D}}, \dot{q}_{3\mathrm{D}}, u_{3\mathrm{D}}) > 0 \right\}.$$

b. Reset Map

As mentioned previously, the transition to the next domain is knee-lock. The unilateral constraint $h_{3\mathrm{D},kl}(q_{3\mathrm{D}})$ leads to the guard

$$\mathcal{G}_{3\mathrm{D},kl} = \Bigg\{ (q_{3\mathrm{D}}^T, \dot{q}_{3\mathrm{D}}^T, u_{3\mathrm{D}}^T)^T \in T\mathcal{Q}_e \times \mathbb{R}^{m_{3\mathrm{D}}} : h_{3\mathrm{D},kl}(q_{3\mathrm{D}}) = 0 \\ \text{and } \frac{\partial h_{3\mathrm{D},kl}(q_{3\mathrm{D}})}{\partial q_{3\mathrm{D}}} \frac{dq_{3\mathrm{D}}}{dt} < 0 \Bigg\}.$$

For this domain, it is desired that, after impact, the stance foot be in flat contact with the ground and that the stance knee and non-stance knee be locked. This suggests the use of the holonomic constraint for flat foot contact as in (2.22) as well as constraints for knee lock as in (2.38) and (2.39). Combining the associated Jacobian matrices gives the necessary constraint:

$$J_{3\mathrm{D}}^{kl\to hs}(q_e) = \begin{bmatrix} J_{flat}^{stt}(q_e) \\ J_{lock}^{stk}(q_e) \\ J_{lock}^{nsk}(q_e) \end{bmatrix}. \tag{4.12}$$

Using the holonomic constraint whose Jacobian matrix is given in (4.12) and the impact model (2.44) results in the reset map $\Delta_{3\mathrm{D}}^{kl\to hs} : T\mathcal{Q}_e \to T\mathcal{Q}_e$ given in (2.46). The relabeling matrix $\mathcal{R}$ is simply the identity matrix; in other words, no relabeling occurs.

4. Domain 4 (hs)

Both knees are locked and there is flat foot contact of the stance foot as in Section II-D-1. These conditions introduce holonomic constraints on the system.

a. Constrained Dynamics

The constraint vector will combine the kinematic constraint for flat foot contact of the stance foot as in (2.22) with kinematic constraints on the angles of the stance knee and non-stance knee as in (2.38) and (2.39) into the following holonomic constraint

$$\boldsymbol{\eta}_{3\mathrm{D},hs} = (\mathcal{Q}_e, L_e, \eta_{3\mathrm{D},hs})$$

The constraint vector $\eta_{3\mathrm{D},hs}(q_{3\mathrm{D}}, \dot{q}_{3\mathrm{D}}, u_{3\mathrm{D}})$ on the kinematics of the system is

$$\eta_{3\mathrm{D},hs}(q_{3\mathrm{D}}, \dot{q}_{3\mathrm{D}}) = \begin{bmatrix} \eta^{sth}_{flat}(q_{3\mathrm{D}}, \dot{q}_{3\mathrm{D}}, u_{3\mathrm{D}}) \\ \eta^{stk}_{lock}(q_{3\mathrm{D}}, \dot{q}_{3\mathrm{D}}, u_{3\mathrm{D}}) \\ \eta^{nsk}_{lock}(q_{3\mathrm{D}}, \dot{q}_{3\mathrm{D}}, u_{3\mathrm{D}}) \end{bmatrix} \tag{4.13}$$

Using the constraint (4.13), the dynamic model is given by (2.10) with $J_{3\mathrm{D},hs}(q_{3\mathrm{D}})$ the Jacobian matrix satisfying $J_{3\mathrm{D},hs}(q_{3\mathrm{D}})\,\dot{q}_{3\mathrm{D}} = \eta_{3\mathrm{D},hs}(q_{3\mathrm{D}}, \dot{q}_{3\mathrm{D}})$ and $F_{3\mathrm{D}}(q_{3\mathrm{D}}, \dot{q}_{3\mathrm{D}}, u_{3\mathrm{D}})$ the constraint force given by (2.15). The corresponding control system is then $\mathcal{FG}_{3\mathrm{D},hs} = (f_{3\mathrm{D},hs}, g_{3\mathrm{D},hs})$ where

$$f_{3\mathrm{D},hs}(q_e, \dot{q}_e) = \begin{bmatrix} \dot{q}_e \\ \mathcal{D}_e^{-1}(q_e)\Big((I - J^T_{3\mathrm{D},hs}(q_e)\Xi(q_e)J_{3\mathrm{D},hs}(q_e)\mathcal{D}_e^{-1}(q_e)) \cdot \\ \quad (\Upsilon_{nc}(q_e, \dot{q}_e) - \mathcal{C}_e(q_e, \dot{q}_e)\dot{q}_e - \mathcal{G}_e(q_e)) - J^T_{3\mathrm{D},hs}(q_e)\Xi(q_e)\dot{J}_{3\mathrm{D},hs}(q_e, \dot{q}_e)\dot{q}_e \Big) \end{bmatrix},$$

$$g_{3\mathrm{D},hs}(q_e) = \begin{bmatrix} \mathbf{0}_{(n\times m)} \\ \mathcal{D}_e^{-1}(q_e)\left(I_n - J^T_{3\mathrm{D},hs}(q_e)\Xi(q_e)J_{3\mathrm{D},hs}(q_e)\mathcal{D}_e^{-1}(q_e)\right) B_e(q_e) \end{bmatrix}, \tag{4.14}$$

with $\Xi(q_e)$ as in (2.17).

The guard for this domain is knee-lock which occurs when the non-stance knee swings to zero degrees and locks. This is realized as the unilateral constraint

$$\mathbf{h}_{3\mathrm{D},hs} = (\mathcal{Q}_e, L_e, \eta_{3\mathrm{D},kl}) \tag{4.15}$$

with $h_{3D,hs} : \mathcal{Q}_e \to \mathbb{R}_0^+$ a scalar, representing the angle of the stance knee. Specifically, $h_{3D,hs}(q_{3D}) = \vartheta_5$.

The constraints (4.9) and (4.11) can be combined to obtain

$$\mathcal{H}_{3D,ts}(q_{3D}, \dot{q}_{3D}, u_{3D}) = \begin{bmatrix} A_{F_{st}}^T(q_{3D}) F_{st}(q_{3D}, \dot{q}_{3D}, u_{3D}) \\ h_{3D,kl}(q_{3D}) \end{bmatrix}$$

This leads to the domain of admissibility

$$\mathcal{D}_{3D,kl} = \left\{ (q_{3D}^T, \dot{q}_{3D}^T, u_{3D}^T)^T \in T\mathcal{Q}_e \times \mathbb{R}^{m_{3D}} : \mathcal{H}_{3D,kl}(q_{3D}, \dot{q}_{3D}, u_{3D}) > 0 \right\}$$

and the guard

$$\mathcal{G}_{3D,kl} = \left\{ (q_{3D}^T, \dot{q}_{3D}^T, u_{3D}^T)^T \in T\mathcal{Q}_e \times \mathbb{R}^{m_{3D}} : h_{3D,kl}(q_{3D}) = 0 \right. \\ \left. \text{and } \frac{\partial h_{3D,kl}(q_{3D})}{\partial q_{3D}} \frac{dq_{3D}}{dt} < 0 \right\}$$

b. Reset Map

As mentioned previously, the transition to the next domain is heel-strike. This is the last domain in a step and, therefore, the legs will be swapped in the transition to the next domain. For this domain, it is desired that, after impact, the non-stance heel be in rolling contact with the ground, that the stance foot begins to roll up about the toe, and that the non-stance knee stays locked. Bare in mind that the non-stance heel strikes the ground, but, after reset, this becomes the stance heel. These conditions suggest the use of a holonomic constraint for rollng foot contact with the stance toe and non-stance heel as in (2.31) as well a constraint for knee lock as in (2.39) on the non-stance knee. Combining the associated Jacobian matrices gives the necessary

constraint:

$$J_{\text{3D}}^{hs\to ts}(q_e) = \begin{bmatrix} J_{roll}^{stt}(q_e) \\ J_{roll}^{nsh}(q_e) \\ J_{lock}^{nsk}(q_e) \end{bmatrix}. \tag{4.16}$$

Using the holonomic constraint whose Jacobian matrix is given in (4.16) and the impact model (2.44) results in the reset map $\Delta_{\text{3D}}^{hs\to ts} : T\mathcal{Q}_e \to T\mathcal{Q}_e$ given in (2.46). The relabeling matrix $\mathcal{R}(q_e)$, which is just a linear transformation, for this domain is the mirror of the identity matrix or $\mathcal{R}(q_e) = \text{antidiag}(\mathbf{1}_n)$ for the choice of coordinates given in Fig. 10.

CHAPTER V

SAGITTAL CONTROL LAWS

The overall goal of this thesis is to achieve bipedal walking in three dimensions. As mentioned previously, the first step will be to apply a *sagittal restriction* to the three-dimensional model, thereby reducing the dimensionality of the system and, more importantly, effectively restricting the system to operate in the sagittal plane. Walking in the sagittal plane is quite easy to achieve in comparison to three-dimensional walking and has been achieved on models with feet using a variety of methods, see, for example, [7, 22, 99]. This chapter will introduce control laws which can be used to obtain walking for the sagitally-restricted model. In Chapter VII, these control laws will be used with additional control laws to migrate this walking to three dimensions.

The Lagrangian of the three-dimensional biped has the general form:

$$L_{3\mathrm{D}}(q_{3\mathrm{D}}, \dot{q}_{3\mathrm{D}}) = \frac{1}{2} \begin{pmatrix} \dot{\vartheta}^T & \dot{\varphi}^T \end{pmatrix} \underbrace{\begin{pmatrix} D_\vartheta(\vartheta,\varphi) & D^T_{\varphi,\vartheta}(\vartheta,\varphi) \\ D_{\varphi,\vartheta}(\vartheta,\varphi) & D_\varphi(\vartheta,\varphi) \end{pmatrix}}_{D_{3\mathrm{D}}(q_{3\mathrm{D}})} \begin{pmatrix} \dot{\vartheta} \\ \dot{\varphi} \end{pmatrix} - V_{3\mathrm{D}}(\vartheta,\varphi) \tag{5.1}$$

where the inertia matrix $D_{3\mathrm{D}}(q_{3\mathrm{D}})$ is in block-form and $V_{3\mathrm{D}}(q_{3\mathrm{D}})$ is the potential energy.

A. Reduced Dynamics

Consider the sagittal dynamics of the three-dimensional biped obtained by applying the sagittal restriction to the three-dimensional model. These dynamics have con-

figuration space $S = \mathbb{R}^{n-m}$ (where m is the number of almost-cyclic variables (these will be defined later) in the three-dimensional system) with coordinates ϑ. The Lagrangian is given by

$$L_{2\mathrm{D}}(\vartheta, \dot{\vartheta}) = \frac{1}{2}\dot{\vartheta}^T D_{2\mathrm{D}}(\vartheta)\dot{\vartheta} - V_{2\mathrm{D}}(\vartheta),$$

with $D_{2\mathrm{D}}(\vartheta) = D_\vartheta(\vartheta, \varphi)|_{\varphi=\mathbf{0}_{(m\times 1)}}$ a submatrix as defined in (5.1) and $V_{2\mathrm{D}}(\vartheta) = V_{3\mathrm{D}}(\vartheta, \varphi)|_{\varphi=\mathbf{0}_{(m\times 1)}}$. These equations yield the control system $(f_{2\mathrm{D}}, g_{2\mathrm{D}})$ as in (2.8).

B. Fundamental Control Laws

This section describes the control laws used to obtain walking on the reduced model; i.e., these control laws give walking in the sagital plan on a two-dimensional biped.

1. Controlled Symmetries

The first law considered is controlled symmetries, motivated by [1]. This controller works by shaping the potential energy of the associated Lagrangian to that of a passive biped walking down a slope. A group action, which effectively "rotates the world", operates on the potential energy V. It was shown in [100] that a kneed walker can walk passively down a slope and further shown in [21] that controlled symmetries gives a stable gait for a kneed walker on flat ground.

Consider the group action $\Psi : \mathbb{S} \times \mathcal{Q} \to \mathcal{Q}$ given by

$$\Psi_\gamma(q) := q + (\gamma, \mathbf{0}_{n-1})^T,$$

for slope angle $\gamma \in \mathbb{S}$, $q \in \mathbb{R}^n$ and $\mathbf{0}_k$ the zero vector of length n. From this, define the feedback control law

$$K^\gamma_{2\mathrm{D}}(q) = B^{-1}(q)\left(G(q) - G(\Psi_\gamma(q))\right), \tag{5.2}$$

where $B(q)$ is a torque distribution map as in (2.4). Note that this control law requires full actuation (i.e., B must be full rank it is must be invertible). Application of this control law to the control system (f, g) given (2.8) yields the modified vector field

$$f^{\gamma}_{2\mathrm{D}}(q, \dot{q}) := f_{2\mathrm{D}}(q, \dot{q}) + g^{\gamma}_{2\mathrm{D}}(q) K^{\gamma}_{2\mathrm{D}}(q)$$

which is simply the vector field associated to the shaped Lagrangian:

$$L_{2\mathrm{D}}\gamma(q, \dot{q}) = \frac{1}{2}\dot{q}^T D(q)\dot{q} - V(\Psi_{\gamma}(q)).$$

2. Spring-Damper Controller

Motivated by the elasticity of the human ankle and the need to keep the foot from spinning freely when not on the ground, a spring-damper controller is considered which creates forces on the system equivalent to those of a linear spring-damper system. Consider j relative angles $\Theta : \mathcal{Q} \to \mathbb{T}^j$ of the system with angular velocities $\dot{\Theta} : T\mathcal{Q} \to \mathbb{R}^j$ and define the feedback control law:

$$K^{\Theta}_{2\mathrm{D}}(q, \dot{q}) = \left[-k_{\Theta}(\Theta(q) - \Theta_0) - c_{\Theta}\dot{\Theta}(q, \dot{q})\right] B_{\Theta}(q), \tag{5.3}$$

with $k_{gainsd} > 0$ a diagonal matrix of corresponding spring constants, $c_{\Theta} > 0$ a diagonl matrix of viscous damping coefficients, Θ_0 the undeflected angles of the springs, and B_{Θ} a torque distribution matrix corresponding to the relative angles $\Theta(q)$; i.e., $B(q) = \frac{\partial \Theta(q)}{\partial q}$. Applying to (f, g) yields

$$f^{\Theta}_{2\mathrm{D}}(q, \dot{q}) = f_{2\mathrm{D}}(q, \dot{q}) + g^{\Theta}_{2\mathrm{D}}(q) K^{\Theta}_{2\mathrm{D}}(q, \dot{q}).$$

3. Scuffing Prevention Controller.

The final control law considered is designed to prevent scuffing. This control law is a simple nonlinear feedback control law introducing an effect similar to gravity, but

with a repulsive force, given by

$$K_{\text{2D}}^{\mathscr{S}} = -\alpha\, e^{-\rho\, h_{\text{nst}}(q)} \tag{5.4}$$

where $\alpha, \rho \in \mathbb{R}$ are positive constants, $h_{\text{nst}} : \mathcal{Q} \to \mathbb{R}$ is the heiht of the non-stance toe, α represents the strength of repulsion and ρ represents the spatial dissipation rate. Applying this controller yields

$$f_{\text{2D}}^{\mathscr{S}}(q) = f_{\text{2D}}(q, \dot{q}) + g_{\text{2D}}^{\mathscr{S}}(q) K_{\text{2D}}^{\mathscr{S}}(q),$$

where the superscript $\mathscr{S}$ is used to represent the set of control gains $\mathscr{S} = \{\alpha, \rho\}$.

C. Two-Dimensional Control Law Construction

In this subsection,a description is given of how the control laws of the previous subsection are implemented in each domain on the sagitally-restricted model. In all domains, the *spring-damper controller* is implemented as this control law would be replaced by a spring-damper system in a physical construct. This control law, therefore, is implemented in both ankles with control input $K_{\text{2D}}^{\Theta}(q_{\text{2D}}, \dot{q}_{\text{2D}})$ as given in (5.3). As mentioned previously, damping forces of the form $F_{\text{nc}} = \Upsilon_{nc}\dot{q}_{\text{2D}}$ will be implemented in this manner.

1. Domain 1 (ts)

In this domain, the system is underactuated because neither foot is flat on the ground—the stance foot is rolling about the heel and the non-stance foot is rolling about the toe. The presence of underactuations prevents the application of controlled symmetries; however, the amount of time spent in this domain is short and, as a result, the system is able to progress through this domain with only the spring-damper

controller as in (5.3). The control law on this domain is as follows:

$$K^{\Theta}_{\text{2D},ts}(q_{\text{2D}}, \dot{q}_{\text{2D}}) = K^{\Theta}_{\text{2D}}(q_{\text{2D}}, \dot{q}_{\text{2D}}). \tag{5.5}$$

Implementing this control law on the system gives the closed-loop vector field

$$f^{\Theta}_{\text{2D},ts}(q_{\text{2D}}, \dot{q}_{\text{2D}}) = f_{\text{2D}}(q_{\text{2D}}, \dot{q}_{\text{2D}}) + g_{\text{2D}}(q_{\text{2D}}) K^{\Theta}_{\text{2D},ts}(q_{\text{2D}}, \dot{q}_{\text{2D}}).$$

2. Domain 2 (tl)

In this domain, the stance foot is flat on the ground, so the system is fully-actuated. Since this domain has full actuation, controlled symmetries can be applied. Additionally, the spring-damper controller is applied. Combining these controllers gives the applicable control law on this domain:

$$K^{\gamma,\Theta}_{\text{2D},tl}(q_{\text{2D}}, \dot{q}_{\text{2D}}) = K^{\gamma}_{\text{2D}}(q_{\text{2D}}) + K^{\Theta}_{\text{2D}}(q_{\text{2D}}, \dot{q}_{\text{2D}}) \tag{5.6}$$

Implementing this control law results in the closed-loop vector field

$$f^{\gamma,\Theta}_{\text{2D},tl}(q_{\text{2D}}, \dot{q}_{\text{2D}}) = f_{\text{2D},tl}(q_{\text{2D}}, \dot{q}_{\text{2D}}) + g_{\text{2D}}(q_{\text{2D}}) K^{\gamma,\Theta}_{\text{2D},tl}.$$

3. Domain 3 (kl)

In this domain, the stance foot is flat on the ground, so the system is fully-actuated. The non-stance foot is off the ground. To prevent the non-stance toe from passing through the ground, the scuffing prevention controller is used. Since this domain has full actuation, controlled symmetries is implemented. And, as in all domains, the spring-damper controller is used. Thus, the control law on this domain is

$$K^{\gamma,\Theta,\mathscr{S}}_{\text{2D},kl}(q_{\text{2D}}, \dot{q}_{\text{2D}}) = K^{\gamma}_{\text{2D}}(q_{\text{2D}}) + K^{\Theta}_{\text{2D}}(q_{\text{2D}}, \dot{q}_{\text{2D}}) + K^{\mathscr{S}}_{\text{2D}}(q_{\text{2D}}). \tag{5.7}$$

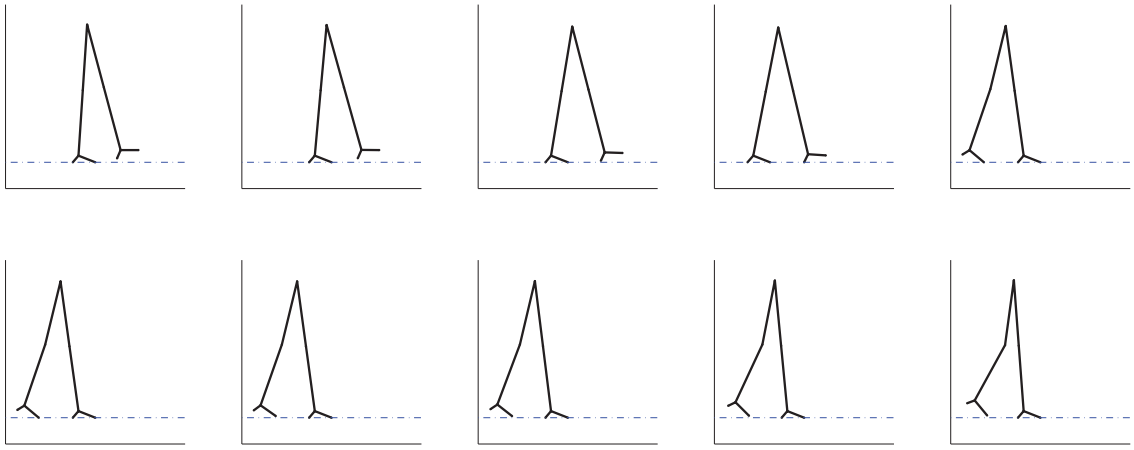

Fig. 11: A stable gait obtained from simulation.

Table I.: Model parameters for biped considered in simulation.

M	.5kg	m_t	.5kg	m_c	50mg	m_f	2.5mg	ℓ	1m
ℓ_t	.175m	ℓ_c	37.5cm	r_h	5cm	r_t	15cm	r_f	5cm
r_a	5cm	γ	.0575rads	k_θ	2Nm/rad	c_θ	.01Nm/rad	θ_0	0°

Applying this control law to the system yields the following closed-loop vector field:

$$f_{2\mathrm{D},kl}^{\gamma,\Theta,\mathscr{S}}(q_{2\mathrm{D}},\dot{q}_{2\mathrm{D}}) = f_{2\mathrm{D},kl} + g_{2\mathrm{D}}(q_{2\mathrm{D}})K_{2\mathrm{D},kl}^{\gamma,\Theta,\mathscr{S}}.$$

4. Domain 4 (hs)

In this domain, the stance foot is flat on the ground. Thus, the system has full actuation and accordingly, controlled symmetries can be applied. The non-stance foot is off the ground so the scuffing prevention controller is used to keep the non-stance toe from passing through the ground. Like the previous domains, this domain also uses the spring-damper controllers. The control law governing this domain is

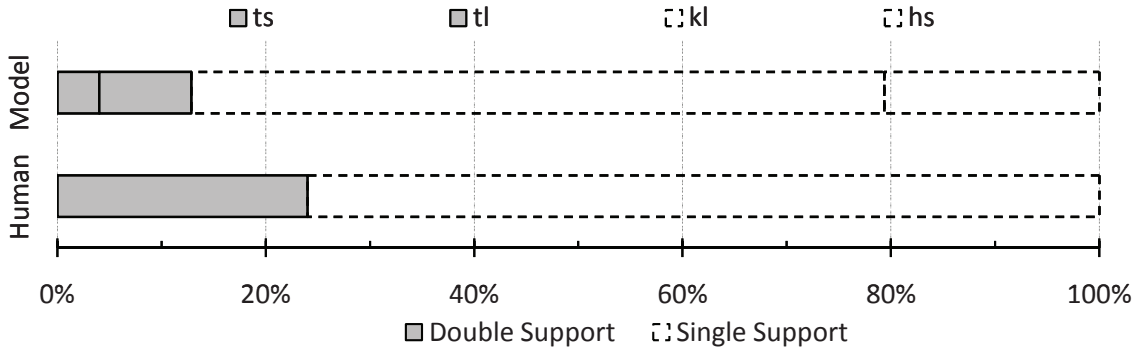

Fig. 12: Temporal breakdown of domains.

given by

$$K^{\gamma,\Theta,\mathscr{S}}_{2\mathrm{D},hs}(q_{2\mathrm{D}},\dot{q}_{2\mathrm{D}}) = K^{\gamma}_{2\mathrm{D}}(q_{2\mathrm{D}}) + K^{\Theta}_{2\mathrm{D}}(q_{2\mathrm{D}},\dot{q}_{2\mathrm{D}}) + K^{\mathscr{S}}_{2\mathrm{D}}(q_{2\mathrm{D}}). \tag{5.8}$$

Imposing this control law gives the closed-loop vector field

$$f^{\gamma,\Theta,\mathscr{S}}_{2\mathrm{D},hs}(q_{2\mathrm{D}},\dot{q}_{2\mathrm{D}}) = f_{2\mathrm{D},hs} + g_{2\mathrm{D}}(q_{2\mathrm{D}})K^{\gamma,\Theta,\mathscr{S}}_{2\mathrm{D},hs}.$$

D. Two-Dimensional Simulation Results

The results of a simulation of a sagitally-restricted biped operating in two dimensions will now be presented. As mentioned earlier, the scuffing prevention controller is applied in domains kl and hs using the parameters $\mathscr{S} = \{\alpha = 1, \rho = 100\}$. The physical parameters used in simulation can be seen in Table I. The simulation started in the domain kl at a fixed point $(q_*^T, \dot{q}_*^T)^T$on the guard $\mathcal{G}_{kl}$.

$$q_{2\mathrm{D},*} = (0.05032 \quad -0.40797 \quad -0.40797 \quad -0.40476)^T,$$
$$\dot{q}_{2\mathrm{D},*} = (1.08454 \quad 0.42106 \quad -8.87553 \quad -8.87555)^T.$$

The gait is shown in Fig. 11 (and a video can be found at [98]). A temporal breakdown of the gait is shown in Fig. 12. One can observe that the majority of the gait is spent in domain ts. This is beneficial because controlled symmetries is

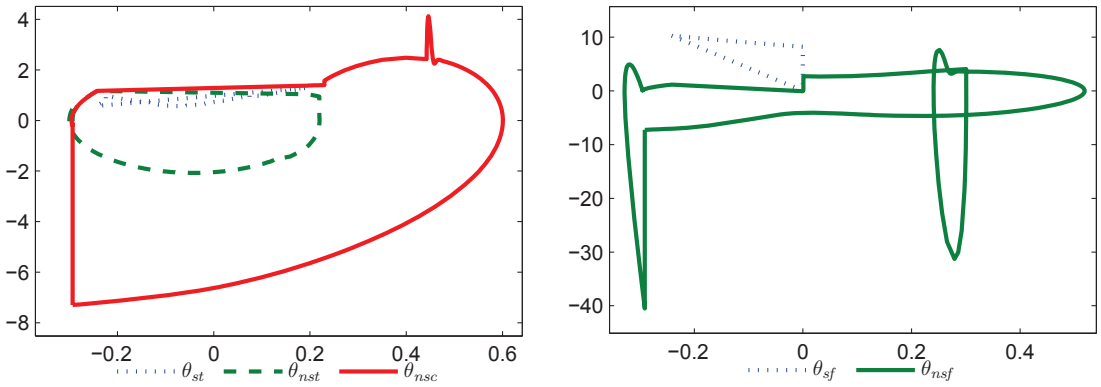

(a) Legs (b) Feet

Fig. 13: Two-dimensional simulation phase portraits with absolute angles.

implemeneted in this domain. In domain kl, no form of control is implemented, and so it is fortunate that this domain is short-lived.

The primary motivation behind adding feet is to allow for the use of controlled symmetries in a realistic model, i.e., a model with underactuation. A system with point feet is necessarily underactuated and is thus incompatible with controlled symmetries. Past research in controlled symmetries has largely considered bipeds with point feet and assumed full actuation [53] in order to develop controlled symmetries. This work shows that controlled symmetries and be expended to bipeds with phases of underactuation. The behavior of the feet through most of the limit cycle does not play a significant role in the gait of the biped. This is supported by the fact that the phase portrait of the legs shown in Fig. 13(a) is qualitatively similar to the phase portrait of a 3D kneed walker without feet as in [21].

The addition of feet introduces a new phenomenon: heel roll. Heel roll occurs when the heel of the non-stance foot strikes the ground before the toe. When this happens, the system is underactuated. Underactuation is undesirable, yet landing on the heel seems to yield a more natural-looking and energy-efficient gait. And so these

events can be effected using the control laws discussed.

It can be seen from Fig. 11 that the non-stance toes stays on the ground until the normal force crosses zero from positive to negative. In other words, the non-stance toe does not go through the ground upon impact. In the majority of the literature (e.g., [8, 53]), an instantaneous double-support phase is considered. The double-support considered in this paper is more realistic and prevents the non-stance toe from passing through the ground (scuffing).

Scuffing occurs when the non-stance foot strikes the ground at an unexpected time. Previous work has largely ignored this problem, yet this problem seems to play an important role in anthropomorphic gaits. That is, a biped must avoid the ground when walking and doing so has an effect on the overall gait. The scuffing prevention controller implemented in this model results in a gait that appears more natural than previous gaits, such as that in [21].

The phase portraits of the various angles are shown in Fig. 13. Note specifically the large angular velocity of the non-stance foot. This occurs for only a short period of time after toe-lift as can be seen from Fig. 14 and is caused by the spring-damper controller and the scuffing prevention controller. Thus, the qualitative behavior of the phase portraits of the feet are heavily dependent upon the parameters chosen for these two controllers.

Fig. 15 shows the Lagrange multipliers at the non-stance toe in domains *ts* and *tl* (in all other domains, the non-stance toe is unconstrained). Discrete transitions are represented by vertical dotted lines (see the figure legend). The important data set to consider is λ_y, which specifies the constraining force at the ground. When this number reaches 0, the *toe-lift* event occurs and the system transitions to domain *kl*. This occurs as a byproduct of the biped's hip and thigh moving forward. It is also interesting to note that the toe would physically remain in contact with the

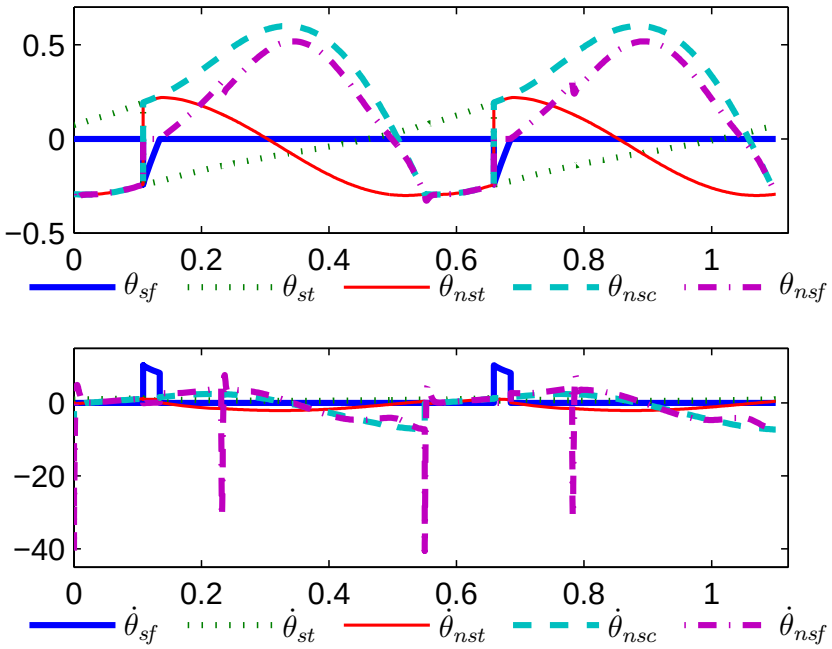

Fig. 14: Two-dimensional state data in absolute angles.

ground since the normal force is positive. Thus, the previous impacts, *heel-strike* and *toe-strike*, should not assume unconstrained movement of the non-stance toe.

One can verify numerically that the limit cycle is locally exponentially stable by examining the eigenvalues of a linearized Poincaré map and calculating the Jacobian at a fixed point by perturbing along the guard. For convenience, choose the Poincaré section to be the guard $\mathcal{G}_{kl}$ which is knee-lock. Since the fixed point is on the guard, there will be $n-1$ eigenvalues, where n is the dimension of the domain. Domain kl has dimension $n=7$ so there are six eigenvalues. The fixed point $x^* = (q_{\text{2D},*}^T, \dot{q}_{\text{2D},*}^T)^T$ which is the initial condition used for the simulation.

The eigenvalues have magnitudes: 0.9526, 0.2761, 0.2761, 0.0023, 1.2520×10^{-4}, 1.7775×10^{-5} and 3.7287×10^{-6}. Note that all these eigenvalues have magnitude less than 1, indicating stability. Further note that number of eigenvalues shown is less than the number of degrees of freedom of the system. This is explained in the

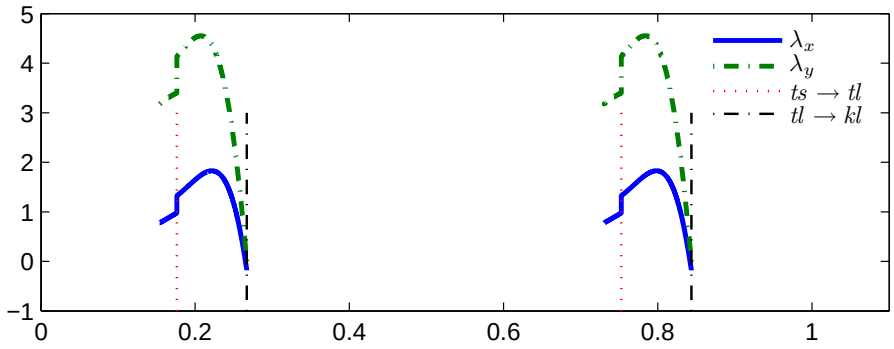

Fig. 15: Lagrange multipliers (x and y).

following remark:

Remark 3. *On hybrid systems with multiple domains, the number of nonzero eigenvalues is limited by the dimension of the appropriate Poincaré section for the domain with the minimum dimension. If the configuration space of this domain is, say, d, then the dimension of the phase space is $2d$ and the number of nonzero eigenvalues is $2d-1$. The dimension is one less than the dimension of the phase space because the Poincaré map is a tranvsere submanifold of the trajectory; in this thesis, the Poincaré section is chosen to be the guard. The rank properties of Poincaré maps are explained in detail in [101].*

CHAPTER VI

FUNCTIONAL ROUTHIAN REDUCTION

One of the primary challenges of bipedal walking introduced by removing the restriction to the sagittal plane (and thereby allowing motion in three dimensions) is the intrinsic coupling between the sagittal and coronal dynamics—this motion is nonlinear and it can be quite difficult to design controllers which result in walking at all let alone anthropomorphic walking. Some work has been done on achieve three-dimensional walking in bipeds (see [40] for a survey). For example, the method of *hybrid zero dynamics* (see [6, 8]) has been used to achieve three-dimensional walking on compass-gait bipeds (see [60]) as well as kneed bipeds (see [39, 41]). Mathematically, the method of hybrid zero dynamics is very elegant and can be optimized for efficiency with respect to specific cost of transport; see [102] for more on the specific cost of transport.

As formal as this method is, it is intuitively complex and does not offer much insight into the fundamental mechanisms that underlie bipedal walking. In this thesis, a variant of geometric reduction—*functional Routhian reduction* (first introduced in [61])—will be used to achieve walking in three dimensions. It will be seen that application of functional Routhian reduction will allow for *decoupling of the sagittal and coronal dynamics* thereby allowing two-dimensional walking to be easily extended to three dimensions. This is very beneficial as it is much easier to achieve anthropomorphic and efficient walking in the sagittal plane than it is to achieve three-dimensional walking.

Functional Routhian reduction, like classical geometric reduction, allows the trajectories of "cyclic" variables to be controlled as the system evolves. However, unlike classical reduction, in which these trajectories are based on a constant *conserved quantity* (generally a momentum), functional Routhian reduction allows the "cyclic" variables to be controlled according to a *functional conserved quantity* or a *momentum map*. This method has been shown to be very effective when used for bipedal walking; to name a few examples, [21, 42].

A. Almost-Cyclic Lagrangians

Consider a system with configuration space $Q = S \times \mathbb{T}^m$, where S is called the *shape space*. Let the coordinates be represented by $q = (\vartheta^T, \varphi^T)^T$ with $\vartheta \in S$ and $\varphi \in \mathbb{T}^m$.

A Lagrangian is $L_\lambda : TS \times TT^m \to \mathbb{R}$ is *almost cyclic* if it takes the form

$$L_\lambda(\vartheta, \varphi, \dot{\vartheta}, \dot{\varphi}) = \frac{1}{2} \begin{bmatrix} \dot{\vartheta}^T & \dot{\varphi}^T \end{bmatrix} D_\lambda(\vartheta) \begin{bmatrix} \dot{\vartheta} \\ \dot{\varphi} \end{bmatrix} - W_\lambda(\vartheta, \varphi, \dot{\vartheta}) - V_\lambda(\vartheta, \varphi) \tag{6.1}$$

with

$$D_\lambda(\vartheta) = \begin{bmatrix} D_\vartheta(\vartheta) + D^T_{\varphi,\vartheta}(\vartheta) D^{-1}_\varphi(\vartheta) D_{\varphi,\vartheta}(\vartheta) & D^T_{\varphi,\vartheta}(\vartheta) \\ D^T_{\varphi,\vartheta}(\vartheta) & D_\varphi(\vartheta) \end{bmatrix}, \tag{6.2}$$

$$W_\lambda(\vartheta, \varphi, \dot{\vartheta}) = \lambda^T(\vartheta) D^{-1}_\varphi(\vartheta) D_{\varphi,\vartheta}(\vartheta) \dot{\vartheta},$$

$$V_\lambda = V_{\text{fct}}(\vartheta) - \frac{1}{2} \lambda^T(\vartheta) D_\varphi(\vartheta) \lambda(\vartheta),$$

for some function $\lambda : \mathbb{T}^m \to \mathbb{R}^m$. Note that $D_\vartheta : S \to \mathbb{R}^{(n-m)\times(n-m)}$ and $D_\varphi : \S \to \mathbb{R}^{m \times m}$ are positive definite and symmetric.

B. Momentum Maps

Reduction is based on the concept of a momentum map, $J : TQ \to \mathbb{R}^m$, which specifies the conserved quantities of a system and is given by

$$J(\vartheta, \varphi, \dot{\vartheta}, \dot{\varphi}) = \frac{\partial L_\lambda}{\partial \dot{\varphi}}(\vartheta, \varphi, \dot{\vartheta}, \dot{\varphi}) = D_{\varphi,\vartheta}(\vartheta)\,\dot{\vartheta} + D_\varphi(\vartheta)\,\dot{\varphi}$$

Unlike standard Routhian reduction, in which the map is a constant, functional Routhian reduction allows us to set this map equal to a function a function $\lambda(\varphi)$.

C. Functional Routhians

For an almost-cyclic Lagrangian L_λ, define the corresponding *functional Routhian* $L_{\text{fct}} : TS \to \mathbb{R}$:

$$L_{\text{fct}}(\vartheta, \dot{\vartheta}) = \Big[L_\lambda(\vartheta, \varphi, \dot{\vartheta}, \dot{\varphi}) - \lambda^T(\varphi)\dot{\varphi}\Big]_{J(\vartheta,\varphi,\dot{\vartheta},\dot{\varphi})=\lambda(\varphi)} \tag{6.3}$$

Because $J(\vartheta, \varphi, \dot{\vartheta}, \dot{\varphi}) = \lambda(\varphi)$ implies that

$$\dot{\varphi} = D_\varphi^{-1}(\vartheta)\left(\lambda(\varphi) - D_{\varphi,\vartheta}(\vartheta)\dot{\vartheta}\right), \tag{6.4}$$

by direct calculation the functional Routhian is given by

$$L_{\text{fct}}(\vartheta, \dot{\vartheta}) = \frac{1}{2}\dot{\vartheta}^T D_\vartheta(\vartheta)\dot{\vartheta} - V_{\text{fct}}(\vartheta). \tag{6.5}$$

Assume there is external forcing of the form $\Upsilon(\vartheta, \dot{\vartheta})$ acting on the ϑ component of the system; that is, $\Upsilon : TS \to \mathbb{R}^{n-m}$. In this case, the vector field can be written as

$$f_{L_\lambda}(q, \dot{q}) = \begin{bmatrix} \dot{q} \\ -D_\lambda^{-1}(q)\left(\mathcal{EL}_q(L_\lambda) - D_\lambda \ddot{q} - \Upsilon(\vartheta, \dot{\vartheta})\right) \end{bmatrix}, \tag{6.6}$$

with $\mathcal{EL}_q(\mathrm{L})$ given in (2.4). In addition, the vector field, $f_{L_{\mathrm{fct}}}$, corresponding to L_{fct} is given by (2.5) and (2.6).

D. Reduction Theorem

Solutions of the forced Lagrangian vector field $f_{L_{\mathrm{fct}}}$ can be related to solutions of the forced Lagrangian vector field f_{L_λ} and vice versa (in a way analogous to the classical Routhian reduction result, see [103]). This fact will now be stated formally:

Theorem 1. *Let L_λ be an almost-cyclic Lagrangian with m almost-cyclic variables and L_{fct} the corresponding functional Routhian with shape space $S = \mathbb{R}^{n-m}$. Additionally, let $\Upsilon : TS \to \mathbb{R}^n$ represent external forcing applied to the system satisfying:*

1. *$\Upsilon(\vartheta, \dot{\vartheta})$ does not depend on $\varphi, \dot{\varphi}$,*
2. *$\Upsilon_i(\vartheta, \dot{\vartheta}) = 0$ for $i = n-m+1, \ldots, n$. (I.e., no external forces act on the angles of the almost-cyclic variables.)*

Then, $(\vartheta(t), \varphi(t), \dot{\vartheta}(t), \dot{\varphi}(t))$ is a solution to the forced vector field f_{L_λ} given by (6.6) *on the interval $[t_0, t_F]$ with*

$$\dot{\varphi}(t_0) = D_\varphi^{-1}(\vartheta(t_0)) \left(\lambda(\varphi(t_0)) - D_{\varphi,\vartheta}(\vartheta(t_0))\, \dot{\vartheta}(t_0) \right), \tag{6.7}$$

if and only if $(\vartheta(t), \dot{\vartheta}(t))$ is a solution to the forced vector field $f_{L_{\mathrm{fct}}}$ given by (2.6) *and $(\varphi(t), \dot{\varphi}(t))$ satisfies:*

$$\dot{\varphi}(t) = D_\varphi^{-1}(\vartheta(t)) \left(\lambda(\varphi(t)) - D_{\varphi,\vartheta}(\vartheta(t))\, \dot{\vartheta}(t) \right). \tag{6.8}$$

Before proving this theorem, some additional information is necessary. First, note that the Lagrangian can be written as

$$L_\lambda(\vartheta, \varphi, \dot{\vartheta}, \dot{\varphi}) = L_{\mathrm{fct}}(\vartheta, \dot{\vartheta}) + \mathrm{Rem}(\vartheta, \varphi, \dot{\vartheta}, \dot{\varphi})$$

with

$$\begin{aligned}\mathrm{Rem}(\vartheta,\varphi,\dot{\vartheta},\dot{\varphi}) = \frac{1}{2}\lambda^T(\varphi)D_{\varphi}^{-1}(\vartheta)\lambda(\varphi) + \frac{1}{2}\dot{\vartheta}^T D_{\varphi,\vartheta}^{t}(\vartheta)D_{\varphi}^{-1}(\vartheta)D_{\varphi,\vartheta}(\vartheta)\,\dot{\vartheta} \\ + \frac{1}{2}\dot{\varphi}^T D_{\varphi}(\vartheta)\,\dot{\varphi} + \dot{\varphi}^T D_{\varphi,\vartheta}(\vartheta)\dot{\vartheta} - \lambda^T(\varphi)D_{\varphi}^{-1}(\vartheta)D_{\varphi,\vartheta}(\vartheta)\,\dot{\vartheta}.\end{aligned}$$

Application of the Euler-Lagrange equations then gives

$$\begin{aligned}\frac{d}{dt}\frac{\partial L_\lambda}{\partial\dot{\vartheta}_i} - \frac{\partial L_\lambda}{\partial\vartheta_i} = \frac{d}{dt}\frac{\partial L_{\mathrm{fct}}}{\partial\dot{\vartheta}_i} - \frac{\partial L_{\mathrm{fct}}}{\partial\vartheta_i} + \frac{d}{dt}\frac{\partial\mathrm{Rem}}{\partial\dot{\vartheta}_i} - \frac{\partial\mathrm{Rem}}{\partial\vartheta_i} = \Upsilon_i(\vartheta,\dot{\vartheta}) \\ \frac{d}{dt}\frac{\partial L_\lambda}{\partial\dot{\varphi}_j} - \frac{\partial L_\lambda}{\partial\varphi_j} = \frac{d}{dt}\frac{\partial\mathrm{Rem}}{\partial\dot{\varphi}_j} - \frac{\partial\mathrm{Rem}}{\partial\varphi_j} = 0\end{aligned}$$

with $i = 1,\ldots,n-m$ and $j = 1,\ldots,m$. The derivatives of Rem are given in Table II.

It will be necessary to show that the Euler-Lagrange equations are satisfied when the functional quantity given in (6.4) is satisfied. This is accomplished through direct substitution. Differentiating (6.4) gives

$$\begin{aligned}\ddot{\varphi} = D_{\varphi}^{-1}(\vartheta)\left(\frac{d}{dt}\left[\lambda(\varphi)\right] - \frac{d}{dt}\left[D_{\varphi,\vartheta}(\vartheta)\right]\dot{\vartheta} - D_{\varphi,\vartheta}(\vartheta)\ddot{\vartheta}\right) \\ - D_{\varphi}^{-1}(\vartheta)\frac{d}{dt}\left[D_{\varphi}(\vartheta)\right]D_{\varphi}^{-1}(\vartheta)\left(\lambda(\varphi) - D_{\varphi,\vartheta}(\vartheta)\dot{\vartheta}\right).\end{aligned} \tag{6.13}$$

Substituting (6.4) and (6.13) into (6.9) and substituting (6.4) into (6.10) yields

$$\begin{aligned}\left.\frac{d}{dt}\frac{\partial\mathrm{Rem}}{\partial\dot{\vartheta}}\right|_{J(\vartheta,\varphi,\dot{\vartheta},\dot{\varphi})=\lambda(\varphi)} = 0, \\ \left.\frac{\partial\mathrm{Rem}}{\partial\vartheta}\right|_{J(\vartheta,\varphi,\dot{\vartheta},\dot{\varphi})=\lambda(\varphi)} = 0.\end{aligned}$$

Similarly, substituting (6.4) and (6.13) into (6.11) and (6.4) into (6.12) and combining the equations yields

$$\left.\frac{d}{dt}\frac{\partial\mathrm{Rem}}{\partial\dot{\varphi}} - \frac{\partial\mathrm{Rem}}{\partial\varphi}\right|_{J(\vartheta,\varphi,\dot{\vartheta},\dot{\varphi})=\lambda(\varphi)} = 0.$$

Table II.: Derivatives of remainder terms in reduction proof.

$$\begin{aligned}
\frac{d}{dt}\frac{\partial \mathrm{Rem}}{\partial \dot{\vartheta}_i} &= \ddot{\vartheta}^T D_{\varphi,\vartheta}^T(\vartheta) D_\varphi^{-1}(\vartheta) D_{\varphi,\vartheta}(\vartheta) e_i + \dot{\vartheta}^T \frac{d}{dt}[D_{\varphi,\vartheta}^T(\vartheta)] D_\varphi^{-1}(\vartheta) D_{\varphi,\vartheta}(\vartheta) e_i \\
&+ \dot{\vartheta}^T D_{\varphi,\vartheta}^T(\vartheta) \frac{d}{dt}[D_{\varphi,\vartheta}^{-1}\vartheta] D_{\varphi,\vartheta}\vartheta e_i + \dot{\vartheta}^T D_{\varphi,\vartheta}^T(\vartheta) D_\varphi^{-1}(\vartheta) \frac{d}{dt}[D_{\varphi,\vartheta}(\vartheta)] e_i \\
&+ \ddot{\varphi} q^T D_{\varphi,\vartheta}(\vartheta) e_i + \dot{\varphi}^T \frac{d}{dt}[D_{\varphi,\vartheta}(\vartheta)] e_i - \frac{d}{dt}[\lambda^T(\varphi)] D_\varphi^{-1}(\vartheta) D_{\varphi,\vartheta}(\vartheta) e_i \\
&- \lambda^T(\varphi) \frac{d}{dt}[D_\varphi^{-1}(\vartheta)] D_{\varphi,\vartheta}(\vartheta) e_i - \lambda^T(\varphi) D_\varphi^{-1}(\vartheta) \frac{d}{dt}[D_{\varphi,\vartheta}(\vartheta)] e_i \qquad (6.9) \\
\frac{\partial \mathrm{Rem}}{\partial \vartheta_i} &= \frac{1}{2}\dot{\vartheta}^T D_{\varphi,\vartheta}^T(\vartheta) \frac{\partial}{\partial \vartheta_i}[D_\varphi^{-1}(\vartheta)] D_{\varphi,\vartheta}(\vartheta)\dot{\vartheta} + \dot{\vartheta}^T D_{\varphi,\vartheta}^T(\vartheta) D_\varphi^{-1}(\vartheta) \frac{\partial}{\partial \vartheta_i}[D_{\varphi,\vartheta}(\vartheta)]\dot{\vartheta} \\
&+ \frac{1}{2}\dot{\varphi}^T \frac{\partial}{\partial \vartheta_i}[D_\varphi(\vartheta)]\dot{\varphi} + \dot{\varphi}^T \frac{\partial}{\partial \vartheta_i}[D_{\varphi,\vartheta}(\vartheta)]\dot{\vartheta} - \lambda^T(\varphi) \frac{\partial}{\partial \vartheta_i}[D_\varphi^{-1}(\vartheta)] D_{\varphi,\vartheta}(\vartheta)\dot{\vartheta} \\
&- \lambda^T(\varphi) D_\varphi^{-1}(\vartheta) \frac{\partial}{\partial \vartheta_i}[D_{\varphi,\vartheta}(\vartheta)]\dot{\vartheta} + \frac{1}{2}\lambda^T(\varphi) \frac{\partial}{\partial \vartheta_i}[D_\varphi^{-1}]\lambda(\varphi) \qquad (6.10) \\
\frac{d}{dt}\frac{\partial \mathrm{Rem}}{\partial \dot{\varphi}_j} &= e_j^T D_\varphi(\vartheta)\ddot{\varphi} + e_j^T \frac{d}{dt}[D_\varphi(\vartheta)]\dot{\varphi} + e_j^T \frac{d}{dt}[D_{\varphi,\vartheta}(\vartheta)]\dot{\vartheta} + e_j^T D_{\varphi,\vartheta}(\vartheta)\ddot{\vartheta} \qquad (6.11) \\
\frac{\partial \mathrm{Rem}}{\partial \varphi_j} &= -\frac{\partial}{\partial \varphi_j}[\lambda^T(\varphi)] D_\varphi^{-1}(\vartheta) D_{\varphi,\vartheta}(\vartheta)\dot{\vartheta} + \frac{\partial}{\partial \varphi_j}[\lambda^T(\varphi)] D_\varphi^{-1}(\vartheta)\lambda(\varphi) \qquad (6.12)
\end{aligned}$$

Thus, the Euler-Lagrange equations become

$$\frac{d}{dt}\frac{\partial L_\lambda}{\partial \dot{\vartheta}} - \frac{\partial L_\lambda}{\partial \vartheta}\bigg|_{J(\vartheta,\varphi,\dot{\vartheta},\dot{\varphi})=\lambda(\varphi)} = \frac{d}{dt}\frac{\partial L_{\mathrm{fct}}}{\partial \dot{\vartheta}} - \frac{\partial L_{\mathrm{fct}}}{\partial \vartheta} = \Upsilon(\vartheta,\dot{\vartheta}), \qquad (6.14)$$

$$\frac{d}{dt}\frac{\partial L_\lambda}{\partial \dot{\varphi}} - \frac{\partial L_\lambda}{\partial \varphi}\bigg|_{J(\vartheta,\varphi,\dot{\vartheta},\dot{\varphi})=\lambda(\varphi)} = 0. \qquad (6.15)$$

Using this background, Theorem 1 can now be proved.

Proof. ($\Rightarrow$) Let $(\vartheta(t), \varphi(t), \dot{\vartheta}(t), \dot{\varphi}(t))$ be a flow of the forced vector field f_{L_λ} given by (6.6) on $[t_o, t_F]$ with $\bar{\vartheta}(t_0) = \vartheta(t_0)$ and $\dot{\bar{\theta}}(t_0) = \dot{\theta}(t_0)$. In addition, let $\bar{\varphi}(t)$ be a curve

satisfying

$$\bar{\varphi}(t_0) = \varphi(t_0),$$
$$\dot{\bar{\varphi}}(t_0) = D_{\varphi}^{-1}(\bar{\vartheta}(t))\left(\lambda(\bar{\varphi}(t)) - D_{\varphi,\vartheta}(\bar{\vartheta}(t))\right)\dot{\bar{\vartheta}}(t).$$

It follows from (6.14) that the curve $(\bar{\vartheta}(t), \bar{\varphi}(t), \dot{\bar{\vartheta}}(t), \dot{\bar{\varphi}}(t))$ satisfies the forced Euler-Lagrange equations corresponding to L_λ and is thus a flow of the forced vector field f_{L_λ} on $[t_0, t_F]$. Moreover, because both curves have the same initial conditions, it follows by uniqueness that

$$(\vartheta(t), \varphi(t), \dot{\vartheta}(t), \dot{\varphi}(t)) = (\bar{\vartheta}(t), \bar{\varphi}(t), \dot{\bar{\vartheta}}(t), \dot{\bar{\varphi}}(t))$$

and therefore $(\vartheta(t), \dot{\vartheta}(t))$ is a flow of the vector field $f_{L_{\text{fct}}}$ on $[t_0, t_F]$ and $\dot{\varphi}(t)$ satisfies (6.8).

($\Leftarrow$) Let $(\vartheta(t), \dot{\vartheta}(t)$ be a flow of the vector field $f_{L_{\text{fct}}}$ on $[t_0, t_F]$ and $(\varphi(t), \dot{\varphi}(t))$ be a pair satisfying (6.8). It follows from (6.14) that the Euler-Lagrange equations for L_λ are satisfied since the curve $(\vartheta(t), \dot{\theta}(t))$ satisfies the Euler-Lagrange equations for L_{fct} by definition and, therefore, $(\vartheta(t), \varphi(t), \dot{\vartheta}(t), \dot{\varphi}(t))$ is a solution to f_{L_λ} on $[t_0, t_F]$ satisfying (6.7). $\square$

CHAPTER VII

REDUCTION CONTROL LAWS

This chapter will introduce *reduction* control laws which will be applied to the three-dimensional hybrid biped model given in (4.1). The control laws for the sagittally-restricted biped, $K^{\delta}_{2\mathrm{D},i\in V}(q_{2\mathrm{D}},\dot{q}_{2\mathrm{D}})$, (with δ a set of control gains on each domain $i \in V = \{ts, tl, kl, hs\}$), defined earlier as (5.5), (5.6), (5.7), and (5.8), which give stable walking for the sagitally-restricted model. Without loss of generality, the domain subscript will be dropped for the rest of this section.

Recall that the Lagrangian of the 3D biped considered in this paper has the general form (on each domain) given by (5.1). The control system associated to this Lagrangian is given in (2.8). Further, recall that application of the sagittal restriction gives the Lagrangian

$$L_{2\mathrm{D}}(\vartheta,\dot{\vartheta}) = \frac{1}{2}\dot{\vartheta}^T D_{2\mathrm{D}}(\vartheta)\dot{\vartheta} - V_{2\mathrm{D}}(\vartheta),$$

with $D_{2\mathrm{D}}(q_{2\mathrm{D}})$ as in (5.1) and $V_{2\mathrm{D}}(q_{2\mathrm{D}}) = V_{3\mathrm{D}}(q_{2\mathrm{D}},\varphi)|_{\varphi=0}$. These equations yield the control system $(f_{2\mathrm{D}}, g_{2\mathrm{D}})$ as in (2.8), (2.16). Applying the existing control law, $K^{\delta}_{2\mathrm{D},i\in V}(q_{2\mathrm{D}},\dot{q}_{2\mathrm{D}})$, yields the dynamical system:

$$f^{\delta}_{2\mathrm{D}}(q_{2\mathrm{D}},\dot{q}_{2\mathrm{D}}) = f_{2\mathrm{D}}(q_{2\mathrm{D}},\dot{q}_{2\mathrm{D}}) + g_{2\mathrm{D}}(q_{2\mathrm{D}},\dot{q}_{2\mathrm{D}})K^{\delta}_{2\mathrm{D},i\in V}(q_{2\mathrm{D}},\dot{q}_{2\mathrm{D}}), \tag{7.1}$$

which will later be specialized to each domain

Having defined the three-dimensional system and its reduced, two-dimensional counterpart, the focus will now shift to shaping the three-dimensional system so

that Theorem 1 can be applied, making it equivalent to the two-dimensional system through reduction. In an attempt to satisfy the conditions of Theorem 1, two control laws will be implemented. The first control law transforms the three-dimensional Lagrangian, L_e, given by (6.1), into an almost-cyclic Lagrangian as in the statement of Theorem 1. The second control law uses hybrid zero dynamics to stabilize to the surface of initial conditions (given by (7.7)) for which the reduction is valid. Combining these control laws with the two-dimensional control law, $K^{\delta}_{\text{2D},i\in V}(q_{\text{2D}}, \dot{q}_{\text{2D}})$, will result in walking for the three-dimensional biped.

A. Fundamental Control Laws

1. Lagrangian Shaping Controller

Having an almost-cyclic Lagrangian makes a system amenable to reduction. This controller, therefore, shapes the Lagrangian of the system into an almost-cyclic Lagrangian. Consider the almost-cyclic Lagrangian $L_\alpha(q_{\text{3D}}, \dot{q}_{\text{3D}})$ given in (6.1), where the function $\lambda(\varphi)$ is chosen to be

$$\lambda(\varphi) = -\alpha\varphi$$

where

$$\alpha = -\text{diag}(\alpha_1, \ldots, \alpha_m)$$

with $\alpha_i > 0 \, \forall i \in [1, m] \cap \mathbb{Z}$ constants specifying the rate of convergence. The subscripts are switched accordingly to represent the new control gain, α.

Let $K^{\delta}_{\text{3D}}(q_{\text{3D}}, \dot{q}_{\text{3D}}) = ((K^{\delta}_{\text{2D}}(q_{\text{2D}}, \dot{q}_{\text{2D}}))^T, \mathbf{0}_{m\times 1})^T$ represent the two-dimensional walking controller in a form which can be applied to the three-dimensional system by padding the control vector with m zeros representing the control inputs on the m

cyclic variables (in this case, two). Then define the feedback control law:

$$K_{3D}^{\alpha,\delta}(q_{3D},\dot{q}_{3D}) = B^{-1}(q_{3D})(\mathcal{C}_{3D}(q_{3D},\dot{q}_{3D})\,\dot{q}_{3D} + \mathcal{G}_{3D}(q_{3D}) \tag{7.2}$$
$$+ \mathcal{D}_{3D}(q_{3D})\mathcal{D}_{\alpha}^{-1}(q_{3D})(K_{3D}^{\delta}(q_{3D},\dot{q}_{3D}) - \mathcal{C}_{\alpha}(q_{3D},\dot{q}_{3D})\,\dot{q}_{3D} - \mathcal{G}_{\alpha}(q_{3D}) + \Upsilon_{nc}(q_{3D},\dot{q}_{3D})).$$

where, as given in (6.2), $\mathcal{D}_{\alpha}(q_{3D},\dot{q}_{3D})$ is the shaped inertia matrix, $\mathcal{C}_{\alpha}(q_{3D},\dot{q}_{3D})$ is the shaped Coriolis matrix, and $\mathcal{G}_{\alpha}(q_{3D}) = \frac{\partial V_{\alpha}(q_{3D})}{\partial q_{3D}}$ with $V_{\alpha}(q_{3D})$ having the potential energy of the 2D system $V_{\text{fct}}(q_{3D}) = V_{2D}(q_{2D})$. Applying this control law yields the dynamical system:

$$f_{3D}^{\alpha,\delta} = f_{3D}(q_{3D},\dot{q}_{3D}) + g_{3D}(q_{3D})K_{3D}^{\alpha,\delta}(q_{3D},\dot{q}_{3D}). \tag{7.3}$$

Let the vector field of the two-dimensional system having control input $K_{2D}^{\delta}(q_{2D},\dot{q}_{2D})$ be represented by $f_{2D}^{\delta}(q_{2D},\dot{q}_{2D})$ as in (7.1). By Theorem 1, we then have the following relationship between the behavior of $f_{3D}^{\alpha,\delta}(q_{3D},\dot{q}_{3D})$ and $f_{2D}^{\delta}(q_{2D},\dot{q}_{2D})$:

Proposition 1. *$(\vartheta(t),\varphi(t),\dot{\vartheta}(t),\dot{\varphi}(t))$ is a solution to the vector field $f_{3D}^{\alpha,\delta}(q_{3D},\dot{q}_{3D})$ on $[t_0,t_F]$ with*

$$\dot{\varphi}(t_0) = -D_{\varphi}^{-1}(q_{3D})(\vartheta(t_0))(\alpha\varphi(t_0) + D_{\varphi,\vartheta}(\vartheta(t_0))\dot{\vartheta}(t_0), \tag{7.4}$$

if and only if $(\vartheta(t),\dot{\vartheta}(t))$ is a solution to the vector field $f_{2D}^{\alpha,\delta}(q_{2D},\dot{q}_{2D})$ and $(\varphi(t),\dot{\varphi}(t))$ satisfies:

$$\dot{\varphi}(t) = -D_{\varphi}^{-1}(\vartheta(t))(\alpha\varphi(t) + D_{\varphi,\vartheta}(\vartheta(t))\dot{\vartheta}(t). \tag{7.5}$$

Thus for initial conditions satisfying (7.4), the dynamics of $\mathscr{HC}_{3D}$ can be effectively decoupled into the sagittal and coronal dynamics with the control law $K_{3D}^{\alpha,\delta}(q_{3D},\dot{q}_{3D})$. Note that this control law, as defined in (7.2), contains the two-dimensional control law, $K_{2D}^{\delta}(q_{2D},\dot{q}_{2D})$. Further, the coronal dynamics evolve accord-

ing to (7.5). Because Proposition 1 requires very specific initial conditions, another controller must be implemented to deal with situations where (7.4) is not satisfied.

2. Zero Dynamics Controller

Reduction effectively decouples the sagittal and coronal dynamics but only when the conditions (7.4) of Proposition 1 are satisfied. Since these conditions may not always be satisfied by implementing only the Lagrangian shaping controller, it is necessary to introduce a second controller to drive the system to the surface where these conditions are satisfied; this will be accomplished using the standard method of input/output linearization. (See [104, ch. 9] for the continuous case and [55, 57] for the hybrid analogue.)

Begin by defining a new control system, $(f_{3\mathrm{D}}^{\alpha,\delta}, g_{3\mathrm{D}})$, with $g_{3\mathrm{D}}(q_{3\mathrm{D}})$ given by

$$g_{\mathcal{ZD}}(q_{3\mathrm{D}}) = g_{3\mathrm{D}}(q_{3\mathrm{D}}) \begin{pmatrix} \mathbf{0}_{(n-m)\times(n-m)} & \mathbf{0}_{(n-m)\times m} \\ \mathbf{0}_{n\times(n-m)} & I_m \end{pmatrix}. \tag{7.6}$$

and $f_{3\mathrm{D}}^{\alpha,\delta}(q_{3\mathrm{D}}, \dot{q}_{3\mathrm{D}})$ given in (7.3). Define the output

$$y(q_{3\mathrm{D}}, \dot{q}_{3\mathrm{D}}) = \dot{\varphi} + D_{\varphi}^{-1}(\vartheta) \left(\alpha\, \varphi + D_{\varphi,\vartheta}(\vartheta)\, \dot{\vartheta} \right).$$

Because this output is a function of $\dot{q}_{3\mathrm{D}}$, it has relative degree one. Having $y(q_{3\mathrm{D}}, \dot{q}_{3\mathrm{D}}) = 0$ would satisfy (7.4). Thus, it is desired to drive the system to the so-called *zero dynamics surface*

$$\mathcal{Z} = \left\{ \begin{bmatrix} q_{3\mathrm{D}} \\ \dot{q}_{3\mathrm{D}} \end{bmatrix} \in T\mathcal{Q}_e : y(q_{3\mathrm{D}}, \dot{q}_{3\mathrm{D}}) = 0 \right\}. \tag{7.7}$$

With this in mind and motivated by the standard method of input/output lineariza-

tion for a relative-degree-one system, define the feedback control law:

$$K_{3\mathrm{D}}^{\varepsilon,\alpha,\delta}(q_{3\mathrm{D}},\dot{q}_{3\mathrm{D}}) = -\left(\mathcal{L}_{g_{\mathcal{ZD}}} y(q_{3\mathrm{D}},\dot{q}_{3\mathrm{D}})\right)^{-1}\left(\mathcal{L}_{f_{3\mathrm{D}}^{\alpha,\delta}} y(q_{3\mathrm{D}},\dot{q}_{3\mathrm{D}}) + \frac{1}{\varepsilon} y(q_{3\mathrm{D}},\dot{q}_{3\mathrm{D}})\right), \quad (7.8)$$

where $\mathcal{L}_{g_{\mathcal{ZD}}} y(q_{3\mathrm{D}},\dot{q}_{3\mathrm{D}})$ is the Lie derivative of $y(q_{3\mathrm{D}},\dot{q}_{3\mathrm{D}})$ with respect to $g_{\mathcal{ZD}}(q_{3\mathrm{D}})$ and $\mathcal{L}_{f_{3\mathrm{D}}^{\alpha,\delta}} y(q_{3\mathrm{D}},\dot{q}_{3\mathrm{D}})$ is the Lie derivative of $y(q_{3\mathrm{D}},\dot{q}_{3\mathrm{D}})$ with respect to $f_{3\mathrm{D}}^{\alpha,\delta}$. Note that $K_{3\mathrm{D}}^{\varepsilon,\alpha,\delta}(q_{3\mathrm{D}},\dot{q}_{3\mathrm{D}})$ is well-defined—specifically, $\mathcal{L}_{g_{\mathcal{ZD}}} y(q_{3\mathrm{D}},\dot{q}_{3\mathrm{D}})$ has a finite inverse—as we examine $\mathcal{L}_{g_{\mathcal{ZD}}} y(q_{3\mathrm{D}},\dot{q}_{3\mathrm{D}})$ numerically. Applying this control law results in the dynamical system:

$$f_{3\mathrm{D}}^{\varepsilon,\alpha,\delta}(q_{3\mathrm{D}},\dot{q}_{3\mathrm{D}}) = f_{3\mathrm{D}}^{\alpha,\delta}(q_{3\mathrm{D}},\dot{q}_{3\mathrm{D}}) + g_{\mathcal{ZD}}(q_{3\mathrm{D}}) K_{3\mathrm{D}}^{\varepsilon,\alpha,\delta}(q_{3\mathrm{D}},\dot{q}_{3\mathrm{D}}). \quad (7.9)$$

B. Three-Dimensional Control Law Construction

In this section, it will be shown how the control laws of the previous section are implemented in each domain on the three-dimensional biped model. In each domain, the sagittal control laws designed previously for the sagitally-restricted two-dimensional biped are used. Assume these control laws are padded with zeros in place of the cyclic variables such that they can be applied to the three-dimensional model; let the resulting control laws be written $K_{3\mathrm{D},i\in V}^{\delta}(q_{3\mathrm{D}},\dot{q}_{3\mathrm{D}})$. The goal is to apply these control laws (on each domain) in addition to applying reduction, to achieve walking for the three-dimensional biped. Note that the system has full actuation of the φ (almost-cyclic) coordinates only in domains *tl*, *kl*, and *hs*; thus, reduction can only be applied in these domains (see Theorem 1).

1. Domain 1 (*ts*)

In Domain 1 (*ts*), the system is underactuated, therefore, it is not possible to implement reduction (see Theorem 1) as the assumptions of reduction are not satisfied;

namely, full actuation is required. Thus, this domain only implements the sagittal control law $K^{\delta}_{3\mathrm{D},ts}(q_{3\mathrm{D}}, \dot{q}_{3\mathrm{D}})$ which, when applied to the control system, results in the closed-loop vector field

$$f^{\delta}_{3\mathrm{D},i}(q_{3\mathrm{D}}, \dot{q}_{3\mathrm{D}}) = f_{3\mathrm{D},i}(q_{3\mathrm{D}}, \dot{q}_{3\mathrm{D}}) + g_{3\mathrm{D},i}(q_{3\mathrm{D}})K^{\delta}_{3\mathrm{D},i}(q_{3\mathrm{D}}, \dot{q}_{3\mathrm{D}}).$$

For the other three domains, reduction will be performed.

2. Domain 2 (tl)

The existing control law $K^{\delta}_{3\mathrm{D},tl}(q_{3\mathrm{D}}, \dot{q}_{3\mathrm{D}})$ is implemented in addition to reduction. Start with the control law $K^{\alpha,\delta}_{3\mathrm{D},tl}$ given in (7.2) which gives the vector field

$$f^{\alpha,\delta}_{3\mathrm{D},tl}(q_{3\mathrm{D}}, \dot{q}_{3\mathrm{D}}) = f_{3\mathrm{D},tl}(q_{3\mathrm{D}}, \dot{q}_{3\mathrm{D}}) + g_{3\mathrm{D},tl}(q_{3\mathrm{D}})K^{\alpha,\delta}_{3\mathrm{D},tl}(q_{3\mathrm{D}}, \dot{q}_{3\mathrm{D}})$$

as in (7.3). Combining this vector field with the control field of (2.8) gives the control system $(f_{3\mathrm{D},tl}, g_{3\mathrm{D},tl})$. Finally the control law $K_{3\mathrm{D},tl}\varepsilon, \alpha, \delta(q_{3\mathrm{D}}, \dot{q}_{3\mathrm{D}})$ as given in (7.8) is implemented which yields the dynamical system:

$$f^{\varepsilon,\alpha,\delta}_{3\mathrm{D},tl}(q_{3\mathrm{D}}, \dot{q}_{3\mathrm{D}}) = f^{\alpha,\delta}_{3\mathrm{D},tl}(q_{3\mathrm{D}}, \dot{q}_{3\mathrm{D}}) + g_{\mathcal{ZD},tl}(q_{3\mathrm{D}})K^{\varepsilon,\alpha,\delta}_{3\mathrm{D},tl}(q_{3\mathrm{D}}, \dot{q}_{3\mathrm{D}}).$$

3. Domain 3 (kl)

The existing control law $K^{\delta}_{3\mathrm{D},kl}(q_{3\mathrm{D}}, \dot{q}_{3\mathrm{D}})$ is implemented in addition to reduction. Start with the control law $K^{\alpha,\delta}_{3\mathrm{D},kl}$ given in (7.2) which gives the vector field

$$f^{\alpha,\delta}_{3\mathrm{D},kl}(q_{3\mathrm{D}}, \dot{q}_{3\mathrm{D}}) = f_{3\mathrm{D},kl}(q_{3\mathrm{D}}, \dot{q}_{3\mathrm{D}}) + g_{3\mathrm{D},kl}(q_{3\mathrm{D}})K^{\alpha,\delta}_{3\mathrm{D},kl}(q_{3\mathrm{D}}, \dot{q}_{3\mathrm{D}})$$

as in (7.3). Combining this vector field with the control field of (2.8) gives the control system $(f_{3\mathrm{D},kl}, g_{3\mathrm{D},kl})$. Finally the control law $K^{\varepsilon,\alpha,\delta}_{3\mathrm{D},kl}(q_{3\mathrm{D}}, \dot{q}_{3\mathrm{D}})$ as given in (7.8) is

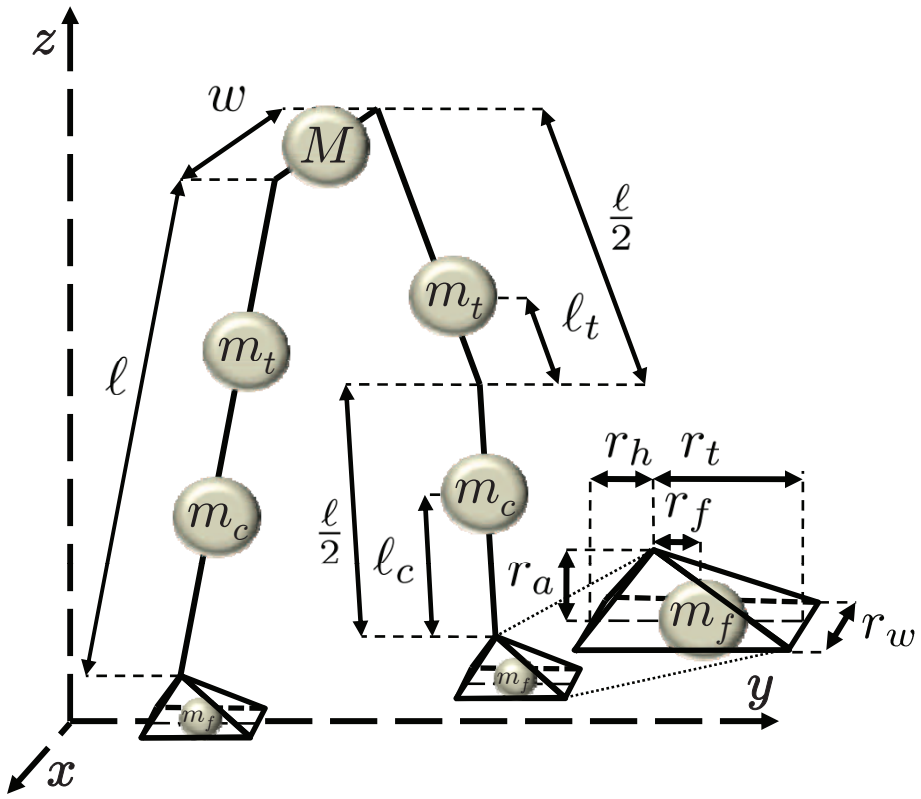

Fig. 16: Physical configuration of 3D model.

implemented which yields the dynamical system:

$$f^{\varepsilon,\alpha,\delta}_{3\mathrm{D},kl}(q_{3\mathrm{D}},\dot{q}_{3\mathrm{D}}) = f^{\alpha,\delta}_{3\mathrm{D},kl}(q_{3\mathrm{D}},\dot{q}_{3\mathrm{D}}) + g_{\mathcal{ZD},kl}(q_{3\mathrm{D}})K^{\varepsilon,\alpha,\delta}_{3\mathrm{D},kl}(q_{3\mathrm{D}},\dot{q}_{3\mathrm{D}}).$$

4. Domain 4 (hs)

The existing control law $K^{\delta}_{3\mathrm{D},hs}(q_{3\mathrm{D}},\dot{q}_{3\mathrm{D}})$ is implemented in addition to reduction. Start with the control law $K^{\alpha,\delta}_{3\mathrm{D},hs}$ given in (7.2) which gives the vector field

$$f^{\alpha,\delta}_{3\mathrm{D},hs}(q_{3\mathrm{D}},\dot{q}_{3\mathrm{D}}) = f_{3\mathrm{D},hs}(q_{3\mathrm{D}},\dot{q}_{3\mathrm{D}}) + g_{3\mathrm{D},hs}(q_{3\mathrm{D}})K^{\alpha,\delta}_{3\mathrm{D},hs}(q_{3\mathrm{D}},\dot{q}_{3\mathrm{D}})$$

as in (7.3). Combining this vector field with the control field of (2.8) gives the control system $(f_{3\mathrm{D},hs}, g_{3\mathrm{D},hs})$. Finally the control law $K_{3\mathrm{D},hs}\varepsilon, \alpha, \delta(q_{3\mathrm{D}}, \dot{q}_{3\mathrm{D}})$ as given in (7.8) is implemented which yields the dynamical system:

$$f^{\varepsilon,\alpha,\delta}_{3\mathrm{D},hs}(q_{3\mathrm{D}}, \dot{q}_{3\mathrm{D}}) = f^{\alpha,\delta}_{3\mathrm{D},hs}(q_{3\mathrm{D}}, \dot{q}_{3\mathrm{D}}) + g_{\mathcal{ZD},hs}(q_{3\mathrm{D}})K^{\varepsilon,\alpha,\delta}_{3\mathrm{D},hs}(q_{3\mathrm{D}}, \dot{q}_{3\mathrm{D}}).$$

5. 3D Simulation Results

The results of a simulation of the three-dimensional biped will now be presented. The physical configuration of the biped is shown in Fig. 16. For this simulation, the model parameters shown in Table I are used.

We perform our simulation starting in domain hs, using the initial condition (on the guard $\mathcal{G}_{3\mathrm{D},hs}$):

$$(q_{3\mathrm{D}})_0 = (4.050\times10^{-4} \quad -2.510\times10^{-4} \quad 0.068 \quad -0.298 \quad -0.298 \quad -1.868)^T,$$
$$(\dot{q}_{3\mathrm{D}})_0 = (3.693\times10^{-3} \quad -1.658\times10^{-3} \quad 0.913 \quad 0.106 \quad -6.130 \quad -6.094)^T.$$

Note that some coordinates are not present as we use model reduction. For example, the stance knee is locked, so the corresponding coordinate is not included.

The gait is shown in Fig. 17 (and a video of the walking can be found at [98]). It is interesting to note that this walking is virtually identical to the two-dimensional gait from Fig. 11. This can be more easily seen by comparing the phase portraits in Fig. 13 and Fig. 18. Because our reduction scheme requires full actuation, it is only possible to implement reduction in domains tl, kl, and hs. Reduction allows us to implement our sagittal control laws and prevents the biped from falling over laterally. This coronal stabilization is not present in domain ts; however, the biped is able to walk as the amount of time spent with (underactuation) is small ($\sim 20\%$) (see Fig. 12).

Because the foot rotation in the coronal plane is small (as can be seen in Fig. 18(c)),

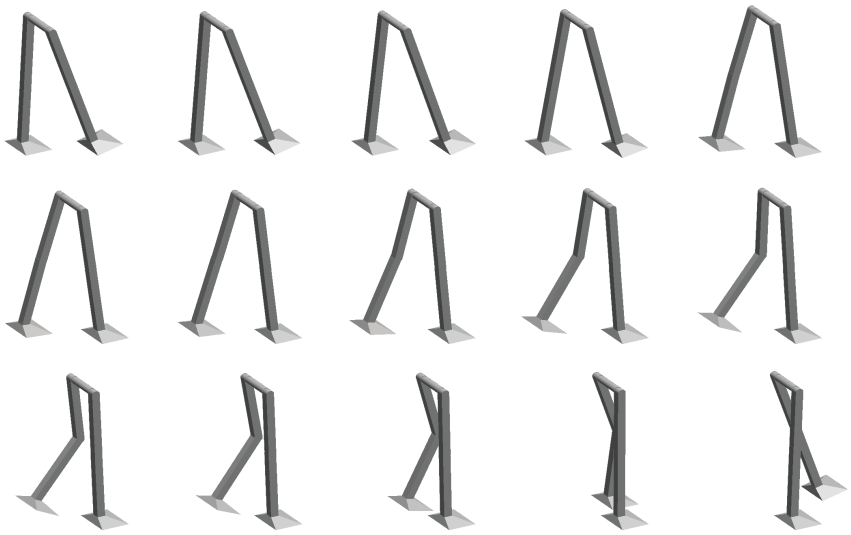

Fig. 17: A gait obtained from simulation.

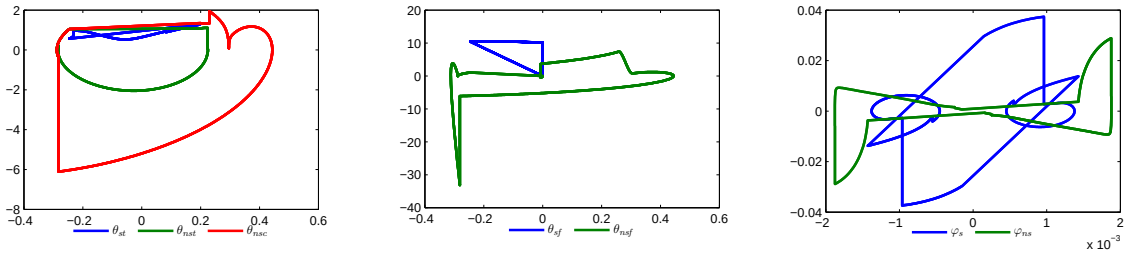

(a) Legs (sagittal) (b) Feet (sagittal) (c) Feet (coronal)

Fig. 18: Phase portraits for three-dimensional simulation with absolute angles.

we make the simplifying assumption that the foot has no coronal rotation when it strikes the ground. This greatly reduces the complexity of the model without significantly affecting its validity. An additional consequence of ignoring foot rotation is that the width of the foot is irrelevant as long as it is not so narrow that the coronal actuation of the ankle and mass distribution of the biped cause the foot to roll on its side. In this paper, the feet are wide enough to negate this concern.

Consider the initial conditions for both the two- and three-dimensional simula-

tions, $q^*_{2\mathrm{D}}$ and $q^*_{3\mathrm{D}}$, respectively. The initial condition for the two-dimensional simulation represents a fixed point of a limit cycle. Thus, given the Poincaré return map $P^{2\mathrm{D}} : TQ_{2\mathrm{D}} \to TQ_{2\mathrm{D}}$ (on a domain) of the two-dimensional system (with $Q_{2\mathrm{D}}$ the configuration space of the two-dimensional model), it is true that $P^{2\mathrm{D}}(q^*_{2\mathrm{D}}) = q^*_{2\mathrm{D}}$. This is simply the definition of a Poincaré map and in fact this is seen from simulation. It is verified through simulation that the same is true of the three-dimensional system—that $P^{3\mathrm{D}}(q^*_{3\mathrm{D}}) = q^*_{3\mathrm{D}}$ given $P^{3\mathrm{D}} : TQ_{3\mathrm{D}} \to TQ_{3\mathrm{D}}$ for configuration space $Q_{3\mathrm{D}}$ (on a domain)—yet stability cannot be numerically verified as in the two-dimensional case due to the extradimensional complexity of the three-dimensional model. However, that the Poincaré return map returns the system to the same point $q^*_{3\mathrm{D}}$ seems to indicate that $q^*_{3\mathrm{D}}$ is, in fact, a fixed point and that the system is stable.

It is interesting to note the similarity between the "fixed points" in both the two- and three-dimensional models. Many of the respective angles are very similar in value. This indicates the effectiveness of functional Routhian reduction as a tool to translate gaits in two-dimensional to gaits in three dimensions. Another metric by which to gauge the efficacy of the reduction is a comparison of phase portraits. Notice the similarities between the two-dimensional phase portraits from Fig. 13 and the three-dimensional phase portraits from Fig. 18. This indicates that the reduction controller seems to operate correctly.

A required condition for Proposition 1 is that the system needs to satisfy (7.4), i.e., the system needs to stabilize to the surface (7.7). In order to drive the system to this surface, we utilize input/output linearization to drive the system to the surface at an exponential rate. The required control decreases as the system approaches the surface. Further, note that the surface is forward invariant and thus no control is needed to stay on the surface.

Consider Fig. 18(c). This figure shows the coronal rotation of the system. Unlike

the two-dimensional system, the three-dimensional systems sways from side-to-side. Thus, the two-dimensional system must go through four domains to return to the fixed point while the three-dimensional system must go through eight domains. In other words, the three-dimensional system is biperiodic. This side-to-side swaying motion is beneficial in that it allows for extra clearance of the non-stance foot as it is swinging. It can also be seen from Fig. 18(c) that the coronal rotation is small ($\approx 10^{-3}$). This is a result of the reduction controller keeping the biped nearly upright in order to satisfy the conditions of Theorem 1.

CHAPTER VIII

CONCLUSIONS

This thesis began by introducing a generalized framework in which to model mechanical systems subject to constraints for which the biped considered is a specific example; the hope is that this framework will be useful in the modeling of a wide range of constrained mechanical systems undergoing impacts. After studying how constraints yield the different components of hybrid systems, a four-domain hybrid model of a bipedal robot was introduced. First, a two-dimensional sagittally-restricted model was considered and stable walking was obtained by using controlled symmetries in the fully-actuated domains combined with local control laws designed to achieve specific objectives. The main theoretical result of this thesis is establishing the validity of functional Routhian reduction in the presence of multiple cyclic variables with external forcing. This result was used with input/output linearization to achieve walking for the three-dimensional biped; in this case, the reduced system obtained through reduction was the two-dimensional sagittally-restricted biped. Finally, a discussion was given on the anthropomorphic nature of the walking with comparison to human data.

Future work includes considering more realistic models, possibly with more domains and higher degrees of freedom. The first step in obtaining even more realistic bipedal models is incorporating more degrees of freedom into the model—especially at the hip. In the case of the biped of interest, there is only one degree of freedom. Finally, some aspects of modeling have been disregarded, e.g., studying the friction

between the foot and the ground. Before constructing a biped, it would be important to test the force of friction to make sure slippage does not occur as well as the other constraints on ground reaction forces and torques mentioned in the modeling section of this thesis.

Additional future work will be directed toward the development of numerical algorithms and simplification of the existing model to accelerate calculations. It was possible to verify stability for the two-dimensional walking by numerically calculating eigenvalues of the Jacobian of the Poincaré map; however, this was not possible for the three-dimensional biped due to computational limitations. Thus, it would be worthwhile to attempt different methods of eigenvalue approximation. A final important topic is the approximation of the domain of attraction of limit cycles in hybrid systems. In general, this is an interesting research problem which would be especially challenging for bipeds due to their high dimensionality. Yet having a metric to quantify system robustness through estimation of the domain of attraction would be invaluable.

REFERENCES

[1] T. McGeer, "Passive dynamic walking," *International Journal of Robotics Research*, vol. 9, no. 2, pp. 62–82, Apr. 1990.

[2] M. W. Spong and F. Bullo, "Controlled symmetries and passive walking," *IEEE Transactions on Automatic Control*, vol. 50, no. 7, pp. 1025–1031, Jul. 2005.

[3] S. H. Collins, A. Ruina, R. Tedrake, and M. Wisse, "Efficient bipedal robots based on passive-dynamic walkers," *Science*, vol. 307, pp. 1082–1085, Feb. 2005.

[4] M. Vukobratović and B. Borovac, "Zero-moment point—thirty-five years of its life," *International Journal of Humanoid Robotics*, vol. 1, no. 1, pp. 157–173, mar 2005.

[5] S. Kajita, F. Kanehiro, K. Kaneko, K. Fujiwara, K. Harada, K. Yokoi, and H. Hirukawa, "Biped walking pattern generator allowing auxiliary ZMP control," in *Proc. of the 2006 IEEE/RSJ International Conference on Intelligent Robots and Systems*, Beijing, P. R. China, Oct. 2006, pp. 2993–2999.

[6] E. R. Westervelt, J. W. Grizzle, and D. E. Koditschek, "Hybrid zero dynamics of planar biped walkers," *IEEE Transactions on Automatic Control*, vol. 48, no. 1, pp. 42–56, Jan. 2003.

[7] C. Chevallereau, D. Djoudi, and J. W. Grizzle, "Stable bipedal walking with foot rotation through direct regulation of the zero moment point," *IEEE Transactions on Robotics*, vol. 25, no. 2, pp. 390–401, Apr. 2008.

[8] E. R. Westervelt, J. W. Grizzle, C. Chevallereau, J. Choi, and B. Morris, *Feed-*

back Control of Dynamic Bipedal Robot Locomotion. Boca Raton, FL: CRC Press, 2007.

[9] T. Reil and P. Husbands, "Evolution of central pattern generators for bipedal walking in a real-time physics environment," *IEEE Transactions on Evolutionary Computation*, vol. 6, no. 2, pp. 159–168, Apr. 2002.

[10] K. Tsuchiya, S. Aoi, and K. Tsujita, "Locomotion control of a biped locomotion robot using nonlinear oscillators," in *IEEE/RSJ International Conference on Intelligent Robots and Systems*, Oct. 2003, pp. 1745–1750.

[11] J. Pratt, P. Dilworth, and G. Pratt, "Virtual model control of a bipedal walking robot," in *IEEE International Conference on Robotics and Automation*, Albuquerque, NM, Apr. 1997, pp. 193–198.

[12] S. Srinivasan, I. A. Raptis, and E. R. Westervelt, "Low-dimensional sagittal plane model of normal human walking," *ASME Journal of Biomechanical Engineering*, vol. 130, no. 5, Oct. 2008.

[13] R. W. Sinnet, M. J. Powell, R. P. Shah, and A. D. Ames, "A human-inspired hybrid control approach to bipedal robotic walking," in *IFAC World Congress*, Milano, Italy, Aug. 2011, preprint available online: http://people.tamu.edu/~rsinnet/papers/ifac_2011_spsa_01.pdf.

[14] M. Ackermann, "Dynamics and energetics of walking with prostheses," Ph.D. dissertation, University of Stuttgart, Stuttgart, Germany, Mar. 2007.

[15] E. Muybridge, *The Human Figure in Motion*, 1st ed. New York, NY: Dover Publications, 1955.

[16] J. Rose and J. G. Gamble, *Human Walking*, 3rd ed. Baltimore, MD: Lippincott Williams & Wilkins, 2005.

[17] P. Saradin and G. Bessonet, "Gait analysis of a human walker wearing robot feet as shoes," in *Proc. of the 2001 IEEE International Conference on Robotics & Automation*, Seoul, Korea, May 2001, pp. 2285–2292.

[18] M. W. Whittle, *An Introduction to Gait Analysis*. Oxford, England: Butterworth-Heinemann, 2005.

[19] D. A. Winter, *Biomechanics and Motor Control of Human Movement*, 2nd ed. New York, NY: Wiley-Interscience, 1990.

[20] A. Goswami, B. Thuilot, and B. Espiau, "A study of the passive gait of a compass-like biped robot: Symmetry and chaos," *International Journal of Robotics Research*, vol. 17, no. 12, pp. 1282–1301, Dec. 1998.

[21] A. D. Ames, R. W. Sinnet, and E. D. B. Wendel, "Three-dimensional kneed bipedal walking: A hybrid geometric approach," in *12th ACM International Conference on Hybrid Systems: Computation and Control, Lecture Notes in Computer Science—HSCC 2009*, R. Majumdar and P. Tabuada, Eds., vol. 5469. San Francisco, CA: Springer-Verlag, Apr. 2009, pp. 16–30.

[22] R. W. Sinnet and A. D. Ames, "2D bipedal walking with knees and feet: A hybrid control approach," in *Proc. of the Joint 48th IEEE Conference on Decision and Control and 28th Chinese Control Conference*, Shanghai, P. R. China, Dec. 2009, pp. 3200–3207.

[23] R. W. Sinnet and A. D. Ames, "Human-inspired autonomous feedback control of bipedal robots," in *Submitted to 50th IEEE Conference on Decision*

and Control, Orlando, FL, Dec. 2011, initial submission available online: http://people.tamu.edu/~rsinnet/msthesis/.

[24] A. Seireg and R. J. Arvikar, "The prediction of muscular load sharing and joint forces in the lower extremities during walking," *ASME Journal of Biomechanics*, vol. 8, pp. 89–102, Mar. 1975.

[25] S. K. Au, P. Dilworth, and H. Herr, "An ankle-foot emulation system for the study of human walking biomechanics," in *IEEE International Conference Robotics and Automation*, Orlando, May 2006, pp. 2939–2945.

[26] M. M. Rodgers, "Dynamic biomechanics of the normal foot and ankle during walking and running," *Physical Therapy*, vol. 68, no. 12, pp. 1822–1830, Dec. 1988.

[27] G. Bergmann, F. Graichen, and A. Rohlmann, "Hip joint loading during walking and running, measured in two patients," *ASME Journal of Biomechanics*, vol. 26, no. 8, pp. 969–990, Aug. 1993.

[28] M. O. Heller, G. Bergmann, G. Deuretzbacher, L. Dürselen, M. Pohl, L. Claes, N. P. Haas, and G. N. Duda, "Musculo-skeletal loading conditions at the hip during walking and stair climbing," *ASME Journal of Biomechanics*, vol. 34, no. 1, pp. 883–893, Jul. 2001.

[29] D. H. Sutherland, K. R. Kaufman, and J. R. Moitoza, "Human walking," in *Kinematics of Normal Human Walking*. Baltimore, MD: Lippincott Williams & Wilkins, 2005, pp. 23–44.

[30] A. G. Bharatkumar, K. E. Daigle, M. G. Pandy, Q. Cai, and J. K. Aggarwal, "Lower limb kinematics of human walking with the medial axis transformation,"

in *IEEE Workshop on Motion of Non-Rigid and Articulated Objects*, Austin, Nov. 1994, pp. 70–76.

[31] V. M.Zatsiorsky, *Kinematics of Human Motion*, 1st ed. Champaign, IL: Human Kinetics, 1997.

[32] S. H. Scott and D. A. Winter, "Biomechanical model of the human foot: Kinematics and kinetics during the stance phase of walking," *ASME Journal of Biomechanics*, vol. 26, no. 9, pp. 1091–1104, Sep. 1993.

[33] U. Glitsch and W. Baumann, "The three-dimensional determination of internal loads in the lower extremity," *ASME J. of Biomech. Eng.*, vol. 30, no. 11, pp. 1123–1131, Nov. 1997.

[34] S. Siegler and W. Liu, "Three-dimensional analysis of human locomotion," in *Inverse Dynamics in Human Locomotion*. New York, NY: John Wiley & Sons, 1997, pp. 191–209.

[35] F. C. Anderson and M. G. Pandy, "Dynamic optimization of human walking," *ASME J. of Biomech. Eng.*, vol. 123, no. 5, pp. 381–390, Oct. 2001.

[36] R. R. Neptune, S. A. Kautz, and F. E. Zajac, "Contributions of the individual ankle plantar flexors to support, forward progression and swing initiation during walking," *J. of Biomech.*, vol. 34, no. 11, pp. 1387–1398, Nov. 2001.

[37] M. G. Pandy and N. Berme, "A numerical method for simulating the dynamics of human walking," *J. of Biomech.*, vol. 21, no. 12, pp. 1043–1051, Apr. 1988.

[38] I. B. Vapnyarskii, "Lagrange multipliers," in *Encyclopaedia of Mathematics*, M. Hazewinkel, Ed. Berlin, Germany: Springer, Jul. 1995.

[39] C. Chevallereau, J. W. Grizzle, and C. Shih, "Asymptotically stable walking of a five-link underactuated 3D bipedal robot," *IEEE Transactions on Robotics*, vol. 25, no. 1, pp. 37–50, Feb. 2009.

[40] J. W. Grizzle, C. Chevallereau, A. D. Ames, and R. W. Sinnet, "3D bipedal robotic walking: Models, feedback control, and open problems," in *Proc. of the 8th IFAC Symposium on Nonlinear Control Systems—NOLCOS 2010*, Bologna, Italy, Sep. 2010.

[41] J. W. Grizzle, C. Chevallereau, and C. Shih, "HZD-based control of a five-link underactuated 3D bipedal robot," in *Proc. of the 47th IEEE Conference on Decision and Control*, Cancún, México, Dec. 2008.

[42] R. W. Sinnet and A. D. Ames, "3D bipedal walking with knees and feet: A hybrid geometric approach," in *Proc. of the Joint 48th IEEE Conference on Decision and Control and 28th Chinese Control Conference*, Shanghai, P. R. China, Dec. 2009, pp. 3208–3213.

[43] S. Kajita, M. Morisawa, K. Harada, K. Kaneko, F. Kanehiro, K. Fujiwara, and H. Hirukawa, "Biped walking pattern generation by using preview control of zero-moment point," in *Proc. of the 2003 IEEE International Conference on Robotics & Automation*, vol. 2, Taipei, Taiwan, Sep. 2003, pp. 1620–1626.

[44] M. Vukobratović, B. Borovac, and V. Potkonjak, "ZMP: A review of some basic misunderstandings," *International Journal of Humanoid Robotics*, vol. 3, no. 2, pp. 153–175, Jun. 2006.

[45] A. Goswami, "Foot rotation indicator (FRI) point: A new gait planning tool to evaluate postural stability of biped robots," in *Proc. of the 1990 IEEE Interna-*

tional Conference on Robotics & Automation, Tsukuba, Japan, May 1990, pp. 47–52.

[46] A. Goswami, "Postural stability of biped robots and the foot-rotation indicator (FRI) point," *International Journal of Robotics Research*, vol. 18, no. 6, pp. 523–533, Jun. 1999.

[47] T. McGeer, "Stability and control of two-dimensional biped walking," Center for Systems Science, Simon Fraser University, Burnaby, B.C., Canada, Tech. Rep., Sep. 1988.

[48] A. D. Kuo, "Stabilization of lateral motion in passive dynamic walking," *International Journal of Robotics Research*, vol. 18, no. 9, pp. 917–930, Sep. 1999.

[49] A. D. Kuo, "Energetics of actively powered locomotion using the simplest walking model," *ASME Journal of Biomechanical Engineering*, vol. 124, pp. 113–120, 2002.

[50] S. O. Anderson, M. Wisse, C. G. Atkeson, J. K. Hodgins, G. J. Zeglin, and B. Moyer, "Powered bipeds based on passive dynamic principles," in *5th IEEE/RAS International Conference on Humanoid Robots*, Dec. 2005, pp. 110–116.

[51] M. Wisse and R. Q. van der Linde, *Delft Pneumatic Bipeds*, ser. Springer Tracts in Advanced Robotics. Berlin, Germany: Springer-Verlag, 2007, vol. 34.

[52] J. W. Grizzle and I. Poulakakis, "Book review: Delft pneumatic bipeds," *IEEE Control Systems Magazine*, vol. 28, no. 4, pp. 99–101, Aug. 2008.

[53] M. W. Spong and F. Bullo, "Controlled symmetries and passive walking," in *Proc. of the 2002 IFAC World Congress*, Barcelona, Spain, Jul. 2002.

[54] D. Pekarek, A. D. Ames, and J. E. Marsden, "Discrete mechanics and optimal control applied to the compass gait biped," in *Proc. of the 46th IEEE Conference on Decision and Control*, New Orleans, LA, Dec. 2007, pp. 5376–5382.

[55] J. W. Grizzle, G. Abba, and F. Plestan, "Asymptotically stable walking for biped robots: Analysis via systems with impulse effects," *IEEE Transactions on Automatic Control*, vol. 46, no. 1, pp. 51–64, Jan. 2001.

[56] F. Plestan, J. W. Grizzle, E. R. Westervelt, and G. Abba, "Stable walking of a 7-DOF biped robot," *IEEE Transactions on Robotics*, vol. 19, no. 4, pp. 653–668, Aug. 2003.

[57] B. Morris and J. W. Grizzle, "A restricted Poincaré map for determining exponentially stable periodic orbits in systems with impulse effects: Application to bipedal robots," in *Proc. of the 44th IEEE Conference on Decision and Control and European Control Conference*, Seville, Spain, Dec. 2005, pp. 4199–4206.

[58] C. Chevallereau, G. Abba, Y. Aoustin, F. Plestan, E. R. Westervelt, C. Canudas-de-Wit, and J. W. Grizzle, "RABBIT: A testbed for advanced control theory," *IEEE Control Systems Magazine*, vol. 23, no. 5, pp. 57–79, Oct. 2003.

[59] B. Morris, E. R. Westervelt, C. Chevallereau, G. Buche, and J. W. Grizzle, "Fast motions symposium on biomechanics and robotics," in *Achieving Bipedal Running with RABBIT: Six Steps toward Infinity*, ser. Lecture Notes in Control and Information Sciences, K. Mombaur and M. Dheil, Eds. Heidelberg, Germany: Springer-Verlag, 2006, pp. 277–297.

[60] C. Shih, J. W. Grizzle, and C. Chevallereau, "Asymptotically stable walking of a simple underactuated 3D bipedal robot," in *Proc. of the 33rd Annual Con-*

ference of IEEE Industrial Electronics (IECON 2007), Taipei, Taiwan, Nov. 2007.

[61] A. D. Ames, "A categorical theory of hybrid systems," Ph.D. dissertation, University of California, Berkeley, Berkeley, CA, May 2006.

[62] A. D. Ames and R. D. Gregg, "Stably extending two-dimensional bipedal walking to three dimensions," in *Proc. of the 26th American Control Conference*, New York, NY, Jul. 2007.

[63] A. D. Ames, R. D. Gregg, and M. W. Spong, "A geometric approach to three-dimensional hipped bipedal robotic walking," in *Proc. of the 45th IEEE Conference on Decision and Control*, San Diego, CA, Dec. 2006.

[64] R. M. Murray, Z. Li, and S. S. Sastry, *A Mathematical Introduction to Robotic Manipulation*. Boca Raton, FL: CRC Press, 1994.

[65] J. Denavit and R. S. Hartenberg, "A kinematic notation for lower-pair mechanisms based on matrices," *ASME Journal of Applied Mechanics*, vol. 23, pp. 215–221, 1955.

[66] R. Featherstone, *Rigid Body Dynamics Algorithms*. New York, NY: Springer, 2007.

[67] M. W. Spong and M. Vidyasagar, *Robot Dynamics and Control*. New York, NY: John Wiley & Sons, 1989.

[68] B. Siciliano, L. Sciavicco, L. Villani, and G. Oriolo, *Robotics: Modelling, Planning and Control*. London, England: Springer, 2008.

[69] J. H. Conway, R. T. Curtis, S. P. Norton, R. A. Parker, and R. A. Wilson, "The groups $\mathbf{GO}_n(q)$, $\mathbf{SO}_n(q)$, $\mathbf{PGO}_n(q)$, $\mathbf{PSO}_n(q)$, and $\mathbf{O}_n(q)$," in *Atlas of*

Finite Groups: Maximal Subgroups and Ordinary Characters for Simple Groups. Oxford, England: Clarendon Press, Jan. 1986, pp. xi–xii.

[70] H. Baruh, *Analytical Dynamics*. New York, NY: WCB/McGraw-Hill, 1998.

[71] R. Courant and D. Hilbert, *Methods of Mathematical Physics*, 1st ed. New York, NY: Wiley-Interscience, 1989, vol. 1.

[72] H. Goldstein, C. P. Poole, and J. L. Safko, *Classical Mechanics*, 3rd ed. San Francisco, CA: Addison-Wesley, 2001.

[73] D. W. Childs, *Dynamics in Engineering Practice (Computation Mechanics and Applied Analysis)*, 10th ed. Boca Raton, FL: CRC Press, 2010.

[74] W. Khalil and E. Dombre, *Modeling, Identification and Control of Robots*. London, England: Hermes Penton Ltd, 2002.

[75] M. W. Spong, S. Hutchinson, and M. Vidyasagar, *Robot Modeling and Control*. New York, NY: John Wiley & Sons, 2005.

[76] B. Torby, *Advanced Dynamics for Engineers*. New York, NY: Holt, Rinehart, and Winston, 1984.

[77] R. S. Ball, *The Theory of Screws: A Study in the Dynamics of a Rigid Body*. Dublin, Ireland: Hodges, Foster, and co., 1876.

[78] R. A. Serway and R. J. Beichner, *Physics for Scientists and Engineers with Modern Physics*, 5th ed. Orlando, FL: Harcourt College Publishers, 1999.

[79] R. N. Jazar, *Theory of Applied Robotics: Kinematics, Dynamics, and Control*, 1st ed. New York, NY: Springer, 2007.

[80] D. A. Suprunenko, "Skew-symmetric matrix," in *Encyclopaedia of Mathematics*, M. Hazewinkel, Ed. Berlin, Germany: Springer, Jul. 1995.

[81] C. Chevallereau, G. Bessonnet, G. Abba, and Y. Aoustin, *Bipedal Robots: Modeling, Design and Walking Synthesis*. New York, NY: Wiley-ISTE, 2009.

[82] M. Vukobratović, B. Borovac, D. Surla, and D. Stokic, *Biped Locomotion*. Berlin, Germany: Springer-Verlag, 1990.

[83] K. Hirai, M. Hirose, Y. Haikawa, and T. Takenaka, "The development of Honda humanoid robot," in *Proc. of the 1998 IEEE International Conference on Robotics & Automation*, Leuven, Belgium, May 1998, pp. 1321–1326.

[84] A. D. Ames, R. Vasudevan, and R. Bajcsy, "Human-data based cost of bipedal robotic walking," in *14th ACM International Conference on Hybrid Systems: Computation and Control*, Chicago, IL, Apr. 2011, pp. 153–162.

[85] B. Brogliato, *Nonsmooth Impact Mechanics: Models, Dynamics, and Control*, 1st ed., ser. Lecture Notes in Control and Information Sciences. New York, NY: Springer, 1996.

[86] V. V. Kozlov and D. V. Treschev, *Billiards: A Genetic Introduction to the Dynamics of Systems with Impacts*, ser. Translations of Mathematical Monographs. Providence, RI: American Mathematical Society, 1991, vol. 89.

[87] D. M. Gorinevsky, A. M. Formal'sky, and A. Y. Schneider, *Force control of robotic systems*, 1st ed. Boca Raton, FL: CRC Press, 1998.

[88] B. Siciliano and L. Villani, *Robot Force Control*, 1st ed., ser. The Springer International Series in Engineering and Computer Science. New York, NY: Springer, 2000.

[89] Q. F. Wei, P. S. Krishnaprasad, and W. P. Dayawansa, "Modeling of impact on a flexible beam," in *Proc. of the 32nd IEEE Conference on Decision and Control*, vol. 2, San Antonio, TX, Dec. 1993, pp. 1377–1382.

[90] Y. Hürmüzlü and D. B. Marghitu, "Rigid body collions of planar kinematic chains with multiple contact points," *International Journal of Robotics Research*, vol. 13, no. 1, pp. 82–92, 1994.

[91] F. Z., *The Schur Complement and Its Applications*, ser. Numerical Methods and Algorithms Series. New York, NY: Springer, 2005, vol. 4.

[92] Y. Or and A. D. Ames, "Stability of Zeno equlibria in Lagrangian hybrid systems," in *Proc. of the 47th IEEE Conference on Decision and Control*, Cancún, México, Dec. 2008.

[93] Y. Or and A. D. Ames, "Existence of periodic orbits in completed lagrangian hybrid systems with non-plastic impacts," in *Hybrid Systems: Computation and Control 2009, Lecture Notes in Computer Science—HSCC 2009*, R. Majumdar and P. Tabuada, Eds., vol. 5469. San Francisco, CA: Springer-Verlag, Apr. 2009, pp. 291–305.

[94] A. Lamperski and A. D. Ames, "On the existence of Zeno behavior in hybrid systems with non-isolated Zeno equilibria," in *Proc. of the 47th IEEE Conference on Decision and Control*, Cancún, México, Dec. 2008, pp. 2776–2781.

[95] R. Goebel, R. Sanfelice, and A. Teel, "Hybrid dynamical systems," *IEEE Control Systems Magazine*, vol. 29, no. 2, pp. 28–93, Apr. 2009.

[96] K. H. Johansson, J. Lygeros, S. N. Simić, J. Zhang, and S. S. Sastry, "Dynami-

cal properties of hybrid automata," *IEEE Transactions on Automatic Control*, vol. 48, no. 1, pp. 2–18, Jan. 2003.

[97] T. S. Parker and L. O. Chua, *Practical numerical algorithms for chaotic systems*. New York, NY: Springer-Verlag, 1989.

[98] R. W. Sinnet, "Ryan Sinnet - Texas A&M M.S. tjhesis," May 2011, http://people.tamu.edu/~rsinnet/msthesis/.

[99] T. Takahashi and A. Kawamura, "Posture control for biped robot walk with foot toe and sole," in *Proc. of the 27th Annual Conference of the IEEE Industrial Electronics Society*, Denver, CO, Dec. 2001, pp. 329–334.

[100] V. F. H. Chen, "Passive dynamic walking with knees: A point foot model," M.S. thesis, Massachusetts Institute of Technology, Cambridge, MA, Feb. 2007.

[101] E. D. B. Wendel and A. D. Ames, "Rank properties of Poincaré maps for hybrid systems with applications to bipedal walking," in *13th ACM International Conference on Hybrid Systems: Computation and Control*, Stockholm, Sweden, Apr. 2010, pp. 151–160.

[102] V. A. Tucker, "The energetic cost of moving about," *American Scientist*, vol. 63, no. 4, pp. 413–419, Jul. 1975.

[103] J. E. Marsden and T. S. Ratiu, *Introduction to Mechanics and Symmetry: A Basic Exposition of Classical Mechanical Systems*, 2nd ed., ser. Texts in Applied Mathematics. New York, NY: Springer, 1999.

[104] S. S. Sastry, *Nonlinear Systems: Analysis, Stability, and Control*, 1st ed. New York, NY: Springer, 1999.

VITA

Name: Ryan Wesley Sinnet

Address: Texas A&M University
Department of Mechanical Engineering
3123 TAMU
College Station, TX 77840-3123

E-mail Address: rsinnet@alumni.caltech.edu

Education: B.S., Electrical Engineering,
California Institute of Technology, 2007
M.S., Mechanical Engineering,
Texas A&M University, 2011

The typist for this thesis was Ryan Wesley Sinnet.